HIGH TEMPERATURE CREEP DEFORMATION OF SILICON NITRIDE CERAMICS

HIGH TEMPERATURE CREEP DEFORMATION OF SILICON NITRIDE CERAMICS

QIANG JIN

B. Eng. and M. Eng. (Tsinghua University)

A Thesis
Submitted to the School of Graduate Studies
in Partial Fullfillment of the Requirements
for the Degree
Master of Engineeering

McMaster University
August 1995

MASTER OF ENGINEERING (1995) McMASTER UNIVERSITY
(Materials Science and Engineering) Hamilton, Ontario

Title: **High Temperature Creep Deformation of Silicon Nitride Ceramics**

Author: Qiang Jin B. Eng. & M. Eng. (Tsinghua University)

Supervisor: Professor D.S.Wilkinson
Professor G.C.Weatherly

Number of Pages: xiv, 102

ABSTRACT

The compressive creep behaviour of a high purity silicon nitride ceramic with and without the addition of Ba was studied at 1400°C. Two distinct creep stages were observed during high temperature deformation of these materials. The stress exponents for creep of the two materials indicate that they have different creep mechanisms during the second stage of creep. Cavitation during creep was determined by measuring the density change before and after creep using a water-displacement method. The Ba doped material exhibited an obvious density decrease, indicating cavitation during creep, whereas the undoped material exhibited no cavitation. This is consistent with TEM observations.

The microstructure of the materials, especially the amorphous grain-boundary phase was investigated for both as-sintered and crept specimans by means of transmission electron microscopy (TEM). Statistical analysis of a number of grain-boundary films indicates that the film thickness is confined to a narrow range (standard deviation less than 0.15 nm) in the as-sintered materials. The average film thickness depends on film chemistry, increasing from 1.0 nm to 1.4 nm when Ba is added. The standard deviation of the film thickness of a given material after

creep, however, is considerably larger than before (0.30 nm ~ 0.59 nm). This suggests that the grain-boundary glass phase is redistributed during creep. Viscous flow of the glass phase is proposed as the mechanism responsible for the first stage of creep. The data are compared with a model for viscous creep, yielding good correlation.

ACKNOWLEDGMENTS

I would like to express my gratitude to my supervisors Professor D.S.Wilkinson and Professor G.C.Weatherly for their constant guidance and advice during this work.

I also wish to thank:

McMaster University and the Department of Materials Science & Engineering for the provision of financial support.

Dr. H.-J. Kleebe of Universitat of Bayreuth, Germany for the provision of experimental materials.

All the students of the mechanical properties group for their friendship and help, especially Ms. Rosaura Ham-Su and Dr. X.-G. Ning for their assistance in creep testing and TEM observations.

Finally, I would like to thank my wife for her understanding and support during the hard times.

TABLE OF CONTENTS

LIST OF FIGURES AND TABLES

CHAPTER 1

INTRODUCTION

Silicon nitride ceramics possess many useful intrinsic properties, e.g. high decomposition temperature, low thermal expansion and high creep resistance, which make them superior to other structural ceramics and commercial high-temperature metallic alloys. Thus, they have received considerable attention in recent years as one of the promising candidates for high temperature applications such as gas turbine engines.

Due to insufficient volume diffusion and volatilization, silicon nitride does not sinter easily in the "pure state". So additions of oxides such as MgO, Y_2O_3 and Al_2O_3 are often used to enhance densification by forming a liquid phase at high temperatures. On cooling, the liquid is usually retained as an intergranular glass phase. The resulting microstructure consists of Si_3N_4 grains, a grain-boundary glass phase and sometimes additional crystalline phase. The creep resistance is limited or decreased when the intergranular glass softens at high temperatures.

Previous work suggests that for glass-containing ceramics such as silicon nitride, creep can occur by viscous flow, dissolution-reprecipitation and cavitation mechanisms. Models have been developed to describe the creep process in terms of the stress and temperature dependence of the creep response based on simple "ideal" microstructures. The creep mechanisms are closely related to the composition and distribution of the intergranular glass phase. However, much of the analysis in the literature is based on empirical relationships. More direct evidence from the microstructural evolution is required in order to fully understand the creep process of silicon nitride. For example, viscous flow controlled creep is generally assumed to be a transient process since the initial intergranular glass phase is very thin, with a thickness in the scale of nanometers. Although several models which capture this essential feature have been developed to describe viscous flow, direct evidence of microstructural evolution due to this process has not been reported.

In the present study, the creep mechanisms of two silicon nitride ceramics were investigated on the basis of creep test data and the observed microstructural evolution. The materials analysed for this work are a high purity silicon nitride and 800 wt. ppm Ba doped silicon nitride. The creep behaviour was evaluated using compression tests. Microstructural observations were conducted by means of

transmission electron microscopy. One objective of this work was to examine the effect of composition of the intergranular glass on the creep mechanisms. A primary point of interest concerns the redistribution of the intergranular phase during creep, evaluated by measuring the thickness of the intergranular glass film before and after creep.

CHAPTER 2

LITERATURE REVIEW

This chapter presents a background of the relevant work in the field of creep of silicon nitride. The first section will introduce the basic microstructural features of silicon nitride, with particular emphasis on the intergranular glass films. The creep behaviour of silicon nitride ceramics, creep models of glass containing ceramics and creep mechanisms of silicon nitride proposed by previous investigators will then be reviewed. Finally, the effect of oxidation and crystallization on creep behaviour will also be described.

2.1 Microstructure and Grain-Boundary Films of Silicon Nitride

Silicon nitride can be considered to be a composite material consisting of elongated β-Si_3N_4 grains embedded in a matrix of glass and finer equiaxed β-Si_3N_4 grains (Wiederhorn et al 1994). This microstructure is determined by the processing techniques. Silicon nitride has strong, directional, covalent bonds which makes the volume diffusivity very low. Densification for pure silicon nitride is therefore very difficult to achieve using classical solid-state sintering techniques. Dense silicon nitride ceramics are invariably sintered using additives which form silicate-related

eutectic liquids based on the SiO_2, which is always present in the starting powder as a surface layer on each silicon nitride particle. It is now recognized that some metal oxides and nitrides (Petzow et al 1981) are effective sintering aids. The sintering liquids usually have M-Si-O-N compositions, herein M indicates the added metallic ion. At high temperatures, this eutectic silica-rich liquid enhances rearrangement of the Si_3N_4 grains. With increasing temperature, the α-Si_3N_4 particles, which are a major component of the starting sintering powders, dissolve in the melt. Upon supersaturation, β-Si_3N_4 is precipitated and either forms small particles in the triple junctions or is epitaxially deposited on pre-existing β-Si_3N_4 particles (Kleebe et al 1994). The resulting microstructure consists of both elongated and finer equiaxed β-Si_3N_4 grains. The elongated grains, with a typical aspect ratio of 5-10 (Lewis et al 1988), can improve the fracture toughness of the silicon nitride (Lange 1973). It is reported (Becher et al 1994) that this can lead to fracture toughness up to 10~12 MPa$\sqrt{m}$ as compared to $\leq$4MPa$\sqrt{m}$ in a fine, more equiaxed grain structure.

Amorphous grain boundary phases are formed upon cooling. These glass phases to a large extent control the high temperature properties of the ceramics. At temperatures exceeding the softening point of the amorphous phases, the diffusion-related behaviour of the material such as creep and oxidation resistance degrade rapidly (Marion et al 1987, Ziegler et al 1987, Cinibulk et al 1992). Therefore

optimization of structural ceramics requires the minimization of the grain-boundary phase and a high viscosity of the sintering liquids. The amount and properties of the glass phase depends on the additives. In general, the amorphous phases are located at multi-grain pockets and along two-grain boundaries. The amorphous secondary phase pockets can be crystallized by heat treatment (Bonnell et al 1987). However, complete crystallization can not be attained as residual glass always remains along two-grain boundaries (Kessler et al 1992). Therefore, the structural and compositional characteristics of the grain-boundary films are thought to be closely related to the reported degradation of the high temperature properties (Pierce et al 1986).

HREM (high-resolution electron microscopy) in combination with AEM (analytical electron microscopy) have provided important information on the grain-boundary film characteristics. Kleebe and co-workers (1993a, 1993b, 1994b, 1994c) have investigated a number of silicon nitride materials, fluxed with various additives, and found that the film thickness at two-grain boundaries is constant within ± 0.1nm for a specific material, independent of grain misorientation. Only small angle grain boundaries and special low energy grain boundaries are not wetted with a glass film (Kleebe et al 1994c). Detailed experimental investigations revealed that silicate-based intergranular films have a thickness between 0.5 and

2.0 nm, depending on the composition of the film. These values of thickness correspond to the stacking of a few SiO_4^{4-} tetrahedra. Although great advances have been made in direct observation of grain-boundary films, the atomic structure of these films is not quite clear. Thorel et al (1986) and Kleebe (1994a) observed ordering at the interface between a Si_3N_4 surface and a SiO_2 glass. It is suggested that ordering exists in the glass adjacent to the interface. On this basis, it is expected that a similar ordering should be observable at the grain-boundary film. However, this could not be revealed so far in a grain-boundary film (Tanaka and Bruley et al 1994).

The constant thickness of grain boundary films has been explained theoretically. Based on the balance of forces acting normal to an intergranular glass film, Clarke and co-workers (1987, 1993) proposed a theory of equilibrium thickness of grain-boundary films. The theory suggests that conditions exist for intergranular phases to exhibit a stable, equilibrium thickness. It is assumed (Clarke 1987) that an equilibrium is established between the attractive van der Waals dispersion force and repulsive forces including a structural disjoining force and an electrical double layer force produced in the amorphous layer. The equilibrium film thickness has also been described by Clarke (1994) using Cahn and Hilliard's (1958) diffuse interface approach.

The film chemistry to a large extent determines the equilibrium film thickness. It is suggested (Kleebe et al 1994c) that the volume fraction of the secondary phase has no major effect on film thickness. Excess glass resides in the triple junctions between grains. The effect of impurity cations on the grain-boundary film thickness has been investigated in several systems. Kleebe et al (1994b) studied Yb_2O_3/Al_2O_3-fluxed Si_3N_4 materials with and without the addition of small amounts of CaO and found that the film thickness increased from 1.0 nm to 1.3 nm with CaO addition. Tanaka et al (1994b) investigated a series of high purity silicon nitride ceramics doped with 0-450 ppm CaO and found that with increasing Ca content the thickness decreased for a dopant of 80 ppm CaO but increased with further additions of CaO, as shown in Fig. 2.1. CaO was selected owing to the extremely limited solubility between CaO and Si_3N_4. It was expected to segregate to the grain-boundary phase, thereby affecting both interface chemistry and the equilibrium film thickness.

Information regarding the composition of the amorphous phase can be obtained by analytical electron microscopy. As mentioned above, the amorphous phase in silicon nitride materials is predominantly composed of silicon, oxygen, nitrogen and sintering additives. The elemental distribution within the amorphous phase has been the topic of extensive composition analysis. Tanaka et al (1994a)

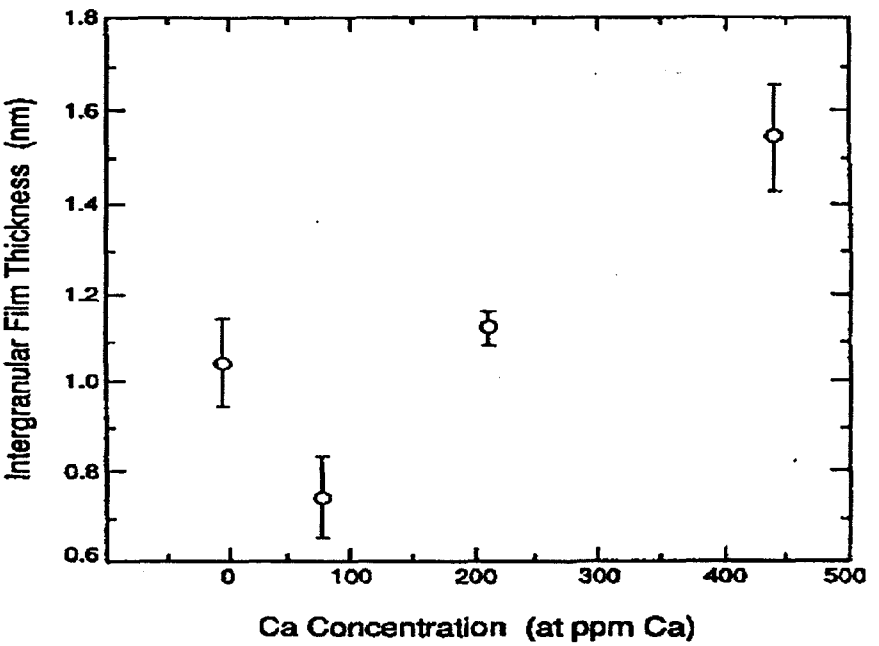

Fig.2.1 Plot of measured film thickness as a function of the Ca content in the silicon ntride materials (Tanaka et al 1994b)

demonstrated that the amorphous grain-boundary film in a Si_3N_4 material is an oxynitride, compositionally graded from nitrogen-rich at the glass-crystal interface to oxygen-rich in the center of the film. The distribution of impurity cations has also been investigated. Kleebe et al (1994b) studied a Ca-doped Si_3N_4 and found that the concentration of Ca is almost constant in the triple junctions and at grain boundaries. However, the composition distribution of impurity cations, such as Ca, across the film thickness has yet to be determined (Tanaka et al 1994a).

2.2 Creep Behaviour of Silicon Nitride

The plastic processes occurring prior to failure at elevated temperatures are referred to as creep. The creep behaviour of silicon nitride depends on many complicated factors, such as the grade of material, the stress and temperature range, and the state of stress (Wilkinson 1994). Generally, three distinct stages are exhibited during creep of materials. After an instantaneous deformation on the application of a load, the creep rate decreases with time during the primary stage, and then remains constant in the stage of steady-state creep. A final (tertiary) stage of creep leads to failure. However, experimental data in the literature suggest that only the first two stages of creep occur in silicon nitride, i.e. primary creep and steady-state creep. In some grades of Si_3N_4, creep consists only of a primary creep

stage (Arons et al 1980, Wiederhorn et al 1993), and failure intervenes before steady-state creep occurs. The absence of tertiary creep is attributed to the lack of long range ductility in structural ceramics (Wiederhorn et al 1994). The classical description of creep may not be applicable for Si_3N_4 ceramics. In analysing the creep behaviour of silicon nitride ceramics, Chadwick and Wilkinson et al (1992, 1993) presented creep test data in terms of creep rate as a function of strain on a log-log plot. Based on this analysis, the concepts of exhaustion creep, steady-state creep and mixed creep were introduced recently by Wilkinson (1994) to classify the creep response of silicon nitride.

The term exhaustion creep describes the creep behaviour whereby an initial period of creep with a relatively constant strain rate is followed by a sharp drop in strain rate when the creep strain reaches a critical value at which creep essentially stops. This phenomenon has been found in four-point bending creep of SN220, a commercial sintered silicon nitride doped with 4% Al_2O_3 and 4% Y_2O_3 (Chadwick 1990), as shown in Fig. 2.2. In other grades of silicon nitride, such as GN10, a commercial material sintered with Y_2O_3 and other additives, under certain testing conditions the creep rate is nearly constant, decreasing very slowly during the entire creep test (Wilkinson 1994). This behaviour is termed steady-state creep. Mixed behaviour is shown in Fig. 2.3 for NT154, a HIPed Y_2O_3-doped silicon

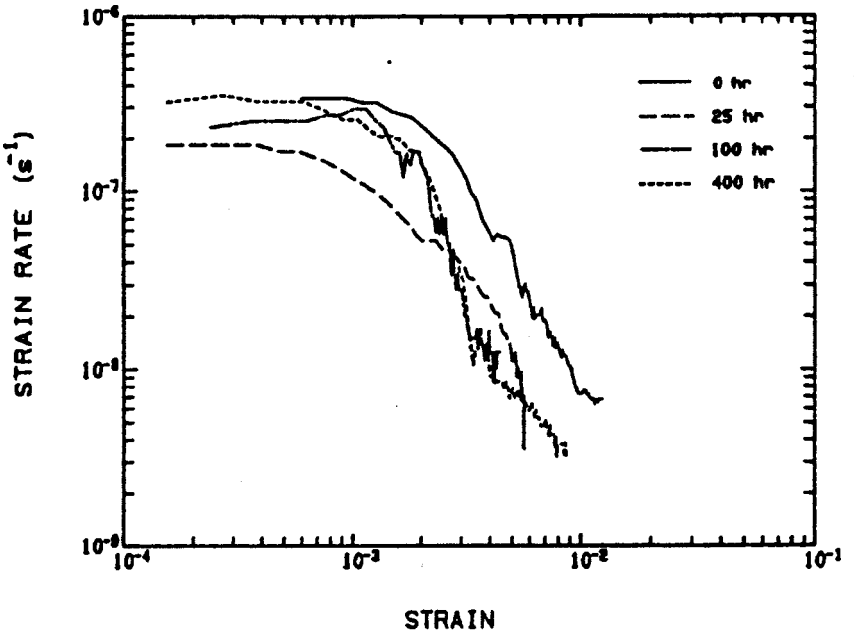

Fig. 2.2 The creep response of SN220 at 1200°C and 63.5MPa under four-point bending. Before creep the material was annealed at 1200°C from 0 to 400h (Chadwick 1990).

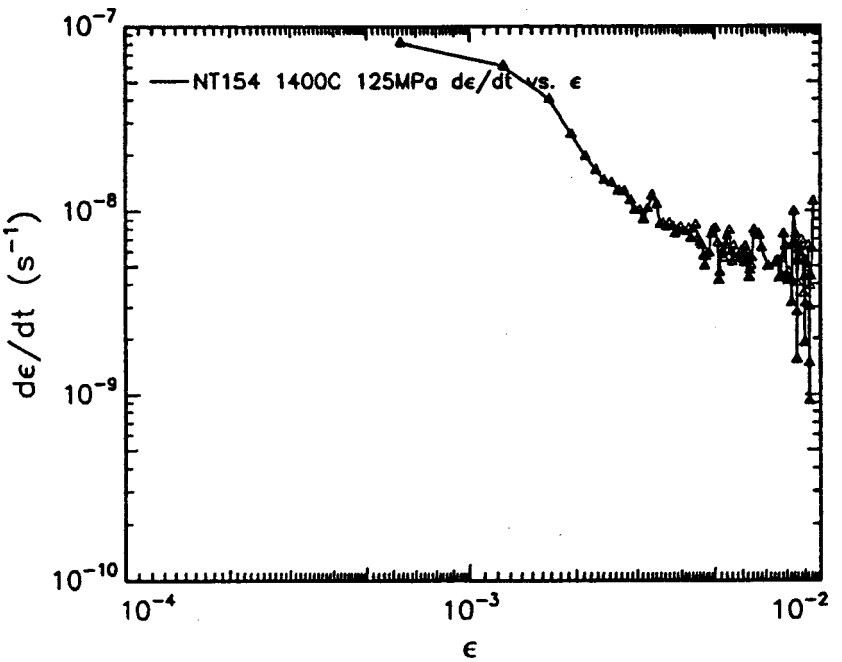

Fig. 2.3 The creep response of NT154 in tension at 1400°C and 125MPa, two plateaus occurring in the creep process (Wilkinson 1994).

nitride. Following a short period of constant creep rate, the creep rate decreases towards a new steady-state rate about one order of magnitude slower (Wilkinson 1994).

It is evident that different materials may have different creep responses. However, the response depends not only on the material, but also on the testing temperature. Fig. 2.4 illustrates the creep curve of SN220, tested at 1325°C in four-point bending (Chadwick 1990); two plateaus occur, which is different from the creep curve shown in Fig. 2.2 for the same material tested at 1200°C, where only one plateau occurs.

Silicon nitride also exhibits creep asymmetry. The creep behaviour in tension and in compression can be totally different. For example, it has been found (Wiederhorn et al 1994) that in NT154 tested at 1430°C, for the same applied stress, the creep rate in tension is from 10 to 100 times greater than that in compression, as shown in Fig. 2.5. This creep asymmetry only occurs in ceramics containing a softer phase at the grain boundaries.

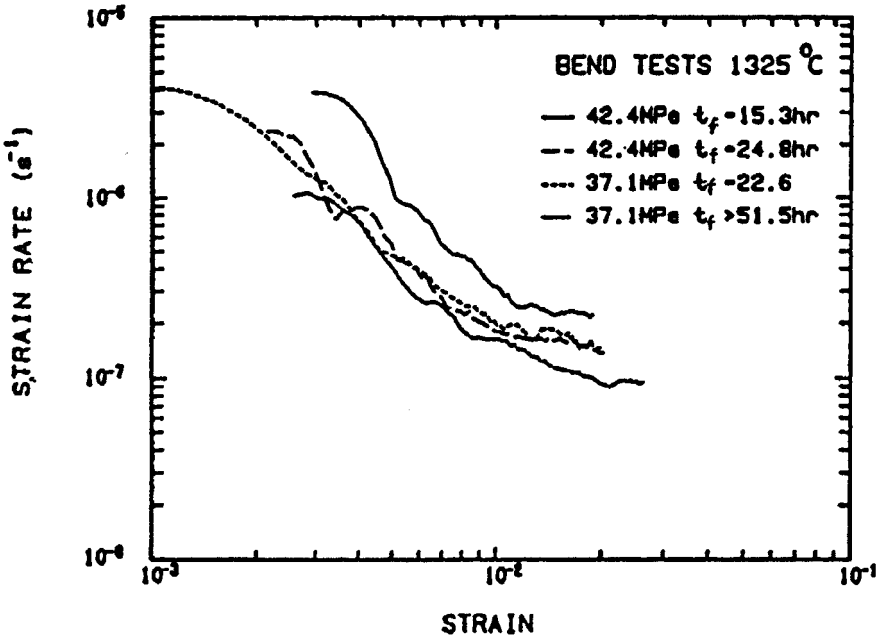

Fig. 2.4 The creep response of SN220 tested in four-point bending at 1325°C. Two plateaus occur during creep, which is different from Fig. 2.2 (Chadwick 1990).

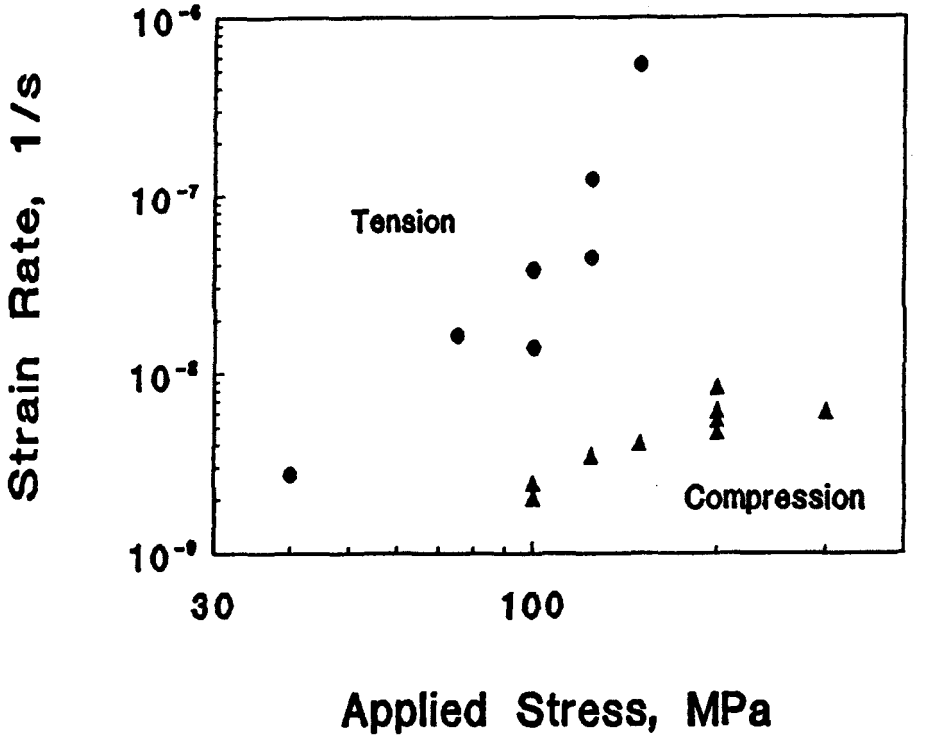

Fig. 2.5 Creep of NT154 at 1430°C, showing creep asymmetry. Under the same applied stress, the creep rate in tension is from 10 to 100 times that in compression (Wiederhorn et al 1994)

2.3 Creep Models for Glass Containing Ceramics

Solid granular materials can creep either by changing the shape of the grains or by grain boundary sliding. If the solid contains an intergranular glass phase which is softer than the solid grains, then it can also creep by flow of the glass phase from one part to another, i.e. redistribution of the intergranular glass phase in the solid (Chadwick et al 1992,1993). Unlike the metallic materials, however, dislocation creep is generally assumed to be negligible in most ceramics, because there is no clear evidence that dislocations are generated or that they move at the creep temperatures (Kossowsky et al 1991, Lange et al 1980b). The commonly accepted view about silicon nitride is that dislocations are immobile at temperatures below 1700°C (Evans et al 1971, Kossowsky 1973). Some investigators, however, have observed dislocations in the crept specimens of silicon nitride. For instance, Tighe (1978) found dislocations in the compressive side of bend bars crept at 1400°C. Din and Nicholson (1975) also found dislocations near voids on the tensile side of bend bars crept between 1200°C ~1400°C. However, even if dislocation motion is possible, TEM studies (Kossowsky 1973) showed that dislocation densities far too low to account for even a small portion of observed strains in crept specimens of silicon nitride. Thus it seems that even though dislocations are active in silicon nitride, there is no evidence that dislocation motion is the dominant creep mechanism. Creep deformation by changing the shape of the grains, therefore, can only occur through a diffusional process. Now it is clear that the creep deformation of glass containing ceramics can occur by several mechanisms, which have been

modelled by previous investigators on the basis of their experimental results, and these are discussed next.

2.3.1 Viscous Flow

In this model, it is assumed that only the viscous glass phase deforms under stress. While the solid grains (e.g. Si_3N_4) do not change shape, relative displacements between the rigid grains can occur. This process is accommodated by flow of the viscous phase from high pressure grain boundaries to low pressure ones. The rate of change in grain boundary thickness will determine the overall creep rate. So far, various models have been presented to describe viscous flow in ceramics containing a glass phase. Among these, a relatively comprehensive model was first proposed by Drucker (1964) using a two dimensional array of hexagons separated by an incompressible fluid, as shown in Fig.2.6. Based on this model, the average strain rate ($\dot{\epsilon}$) is given by

$$\dot{\varepsilon}=\frac{\sigma}{\eta\sqrt{3}}\left(\frac{H}{L}\right)^3 \tag{2.1}$$

where σ is the far field applied stress, 2L the grain facet length, 2H the bonding phase thickness, and η is the viscosity of the bonding phase.

Drucker's model can only be applied at zero strain when the glass layer thickness is equal on all facets. Dryden et al (1989) therefore extended the model by

considering the strain dependence of the creep rate for linear viscous flow. Recently, this model was further developed to include non-linear viscous flow (Chadwick and Wilkinson et al 1992, 1993, Dryden and Wilkinson 1995). The strain rate due to viscous flow is found to be (Dryden and Wilkinson 1995)

$$\dot{\epsilon}=\dot{\epsilon}_o\left[\frac{|\sigma|}{\sigma^*}\right]^n S(\epsilon_N) \tag{2.2}$$

where

$$\sigma^*=\frac{2n(1+2^{1/n})}{3(2n+1)}\left[\frac{2^{n+1}(n+2)}{3^{(n+1)/2}}\right]^{1/n}\frac{\sigma_o}{f^{(n+2)/n}};\quad S(\epsilon_N)=(1+2^{1/n})^n\frac{(1+2\epsilon_N)^{n+2}(1-\epsilon_N)^{n+2}}{[(1+2\epsilon_N)^{(n+2)/n}+2^{1/n}(1-\epsilon_N)^{(n+2)/n}]^n}$$

Here ϵ_N is the normalized strain equal to ϵ/f, and f is the normalized glass layer thickness at zero strain ($f=2H/\sqrt{3}L$), and $\dot{\epsilon}_o$, σ_o and n are material constants. When $n=1$, $\sigma_o=1/\eta$, representing the result for a Newtonian glass.

The predicted strain rate behaviour due to linear and non-linear viscous flow (for n=1, 2, and 3) is shown in Fig. 2.7. The model predicts a nearly constant strain rate at low strains followed by a rapid decrease in strain rate as the maximum strain is reached. Similar creep behaviour is expected for tension and bending using this model. During the viscous flow process, the strain is accumulated as fluid is squeezed out of the compressive interfaces. When the adjacent approaching grains eventually become interlocked, creep due to viscous flow essentially stops.

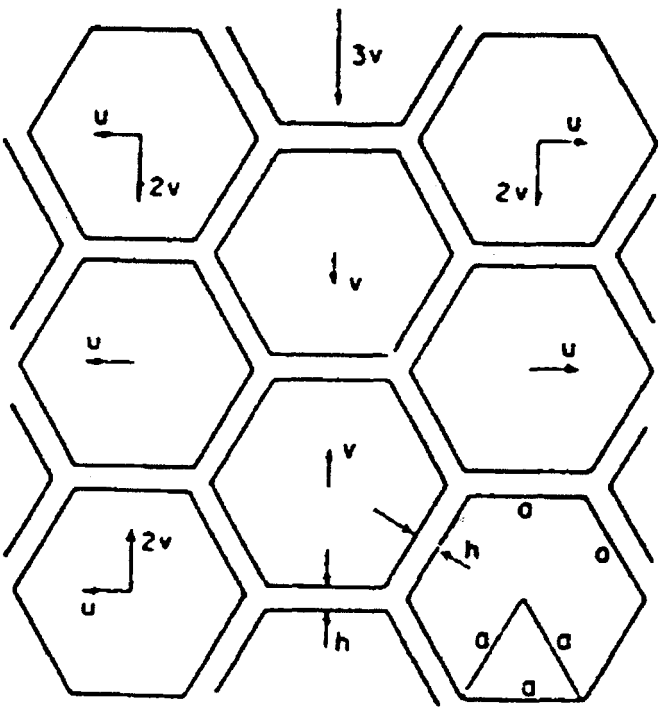

Fig. 2.6 Two dimensional model for incompressive fluid between rigid hexagons (Drucker 1964).

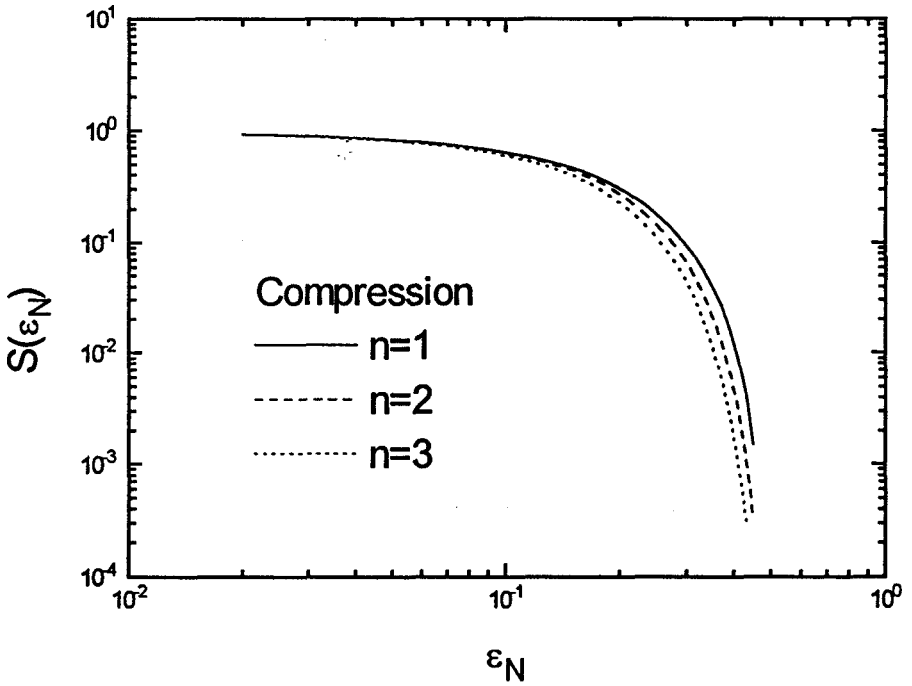

Fig. 2.7 Strain dependence term of the creep rate $S(\epsilon_N)$ as a function of normalized strain $\epsilon_N=\epsilon/f$ predicted theoretically from equation 2.2.

According to this model, the maximum strain equals the fraction of intergranular viscous phase in tension and half that value in compression. This creep asymmetry is inherent in glass containing ceramics because in a microstructure composed of, for simplicity, cubic grains, 2/3 of the grain boundaries can receive glass during compression, but only 1/3 can during tensile creep.

2.3.2 Dissolution-Reprecipitation

This model ascribes the creep deformation of polycrystalline ceramics that contain a residual glass phase to material transport through the glass phase. The diffusional creep in single phase polycrystalline materials has been widely discussed in the literature (Herring 1950, Coble 1963). If there is a liquid phase present in the grain boundaries, in which the grains are partly soluble, then deformation could occur by diffusional transport if the rate of dissolution and reprecipitation is rapid enough (Durney 1972). Furthermore, a fast path of transport through the glass phase at the grain boundary favours Coble creep (Coble 1963) over Nabarro-Herring (Nabarro 1948, Herring 1950) creep as a deformation mechanism. Thus it is reasonable to attribute the deformation caused by solution-reprecipitation in glass-containing ceramics to Coble creep, but with grain boundary diffusion replaced by diffusion through the second phase.

The solution-reprecipitation process has been investigated in a variety of systems (Pharr and Ashby 1983, Raj and Chyung 1981). Pharr and Ashby (1983) found that creep of porous KCl saturated with an aqueous solution is accelerated when there is solubility of the solid in the liquid. The strain rate varies linearly with stress and increases exponentially with temperature. Raj and Chyung (1981) investigated the creep behaviour of a glass ceramic and obtained similar results. Clearly, in this model, the rate of creep is proportional to the rate of solution/reprecipitation, which can be limited either by the interface reaction kinetics or the transport through glass. In the second case, the constitutive equation for creep rate is given by

$$\dot{\varepsilon}=\frac{Kc\sigma H}{L^3\eta} \tag{2.3}$$

where K is a constant, c is the molar fraction of the diffusing species in the glass.

The driving force for matter transport depends on the existence of a gradient of the normal traction along the surface of a grain. In other words, maintaining the pressure differentials is required for the solution/reprecipitation process. Another precondition for this process is the existence of a grain boundary phase. Clarke (1987) has established a theory of equilibrium thickness of the intergranular films.

According to this theory, even under an applied compressive stress, a stable intergranular film will exist. Therefore, the thin layers of glass can support any state of stress and allow for diffusive flow of the solid through them.

2.3.3 Cavitation

The experimental basis of this model is the occurrence of extensive cavitation in the intergranular glass phase during both tensile and compressive creep (Lange et al 1980b, Clarke et al 1985, Jakus et al 1986, Marion et al 1983). Small cavities may develop at the triple pockets and at two-grain interfaces. These can grow along the two-grain interfaces and form microcracks (i.e. full facet cavities according to Marion et al 1983). It is generally assumed that coalescence of microcracks can form cracks. The cracks so formed continue to grow under the applied stress, and creep failure ultimately occurs from one of these cracks. Alternatively, instead of forming cracks, cavities can lead to the accumulation of substantial strains which trigger failure (Wiederhorn et al 1994).

The theoretical analysis of creep due to cavitation has been treated by Marion et al (1983) and Tsai and Raj (1982). For cavity nucleation, time is also required in addition to the critical stress. The time for cavity nucleation and microcrack formation, and crack growth rate determine the lifetime to failure. Expressions

have been developed by Tsai and Raj (1982) to describe the nucleation and growth of cavities. Marion et al (1983) calculated the critical nucleation stresses for spherical cavities at triple junctions and oblate cavities along two-grain boundaries. The critical stress predicted by the model is often greater than the applied far field stress; however, this may be obtained by grain boundary sliding. Grain boundary sliding can cause dilation of the interstitial free spaces in a granular solid. Thus, a negative pressure may develop within the intergranular phase which fills these spaces in glass-containing ceramics. On the other hand, grain boundary sliding can also induce very high transient tensile stresses on some grain boundaries. Page et al (1987) found that in liquid phase sintered alumina the cavity spacing after creep corresponds to that for grain boundary ledges, suggesting the ledges act as nucleation sites.

The process for cavity growth is depicted in Fig. 2.8 (Marion et al 1983). If the stress is high enough to nucleate cavities within two-grain interfaces, full-facet cavities develop by the growth and coalescence of the oblate cavities. If the stress is below that required to nucleate cavities on two-grain boundaries, but above that needed to nucleate cavities within triple pockets, then cavity growth occurs by the viscous flow of the glass phase into the adjacent two grain channels, or by solution/reprecipitation of the solid phase from the cavity surface to the grain

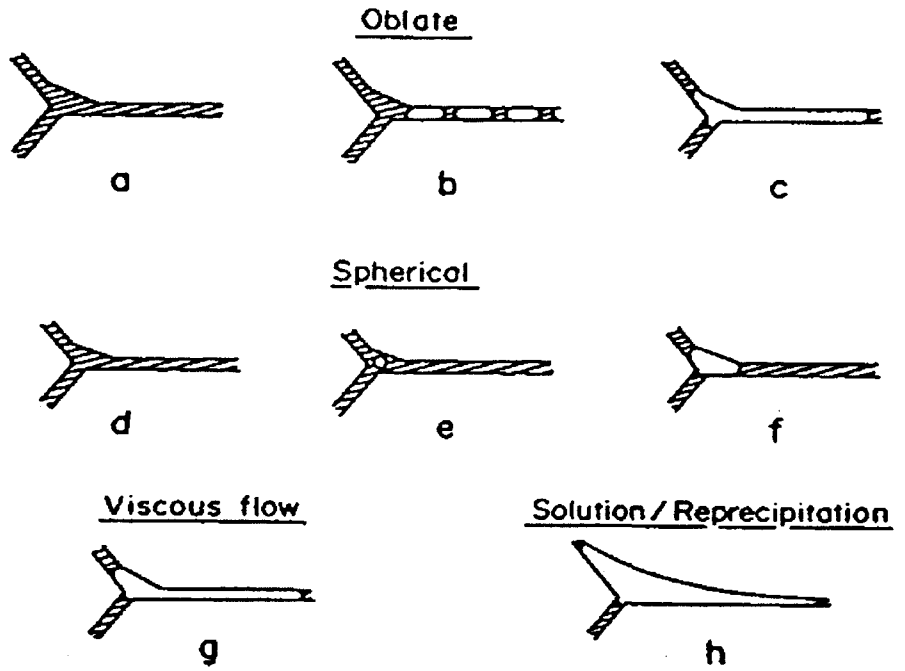

Fig. 2.8 Schematic diagram illustrating the microcrack formation process. (a) uncavitated interface, (b) nucleation of oblate cavities along two-grain boundary, (c) coalescence to a full-facet microcrack, (d) an uncavitated triple pocket, (e) nucleation of a spherical cavity in the glass, (f) depletion of the pocket by viscous flow, (g) expansion to full-facet microcrack by viscous flow, (h) growth to full-facet size by solution-reprecipitation at low stress (Marion et al 1983).

surface within the channel. In the second case, cavities larger in size than the original grain pockets are expected, and this has been observed in silicon nitride and alumina (Marion et al 1983, Clarke 1985).

In this model, it is assumed that cavitation and the accompanying dilation of the material result in a strain rate. Each cavity gives an increment of strain to the total creep deformation. The strain rate depends on the rate of cavitation nucleation and growth. According to Wiederhorn et al (1994), cavitation occurs at the most highly stressed area, relaxing the stress locally and transferring it by grain boundary sliding to some other areas in the structure. The rate of grain boundary sliding is supposed to determine the rate at which cavitation occurs in the solid. With continuing creep, the strain accrues with an increase in the fraction of cavitation.

2.4 Creep Mechanisms Proposed for Silicon Nitride

Since silicon nitride is a glass containing ceramic, the creep models discussed above are all possibly responsible for its creep behaviour. However, it seems difficult to explain the typical creep curve (as shown in Figs. 2.2-2.4) using a single mechanism. The occurrence of steady-state creep after exhaustion creep indicates at least two creep mechanisms must be involved. It is now generally accepted that exhaustion creep is due to viscous flow of the amorphous grain

boundary phase, whereas steady-state creep is due to a combination of cavity growth and dissolution/reprecipitation creep.

The curves of strain rate versus strain predicted by the viscous flow model are consistent with the initial part of creep curves in some materials (compare Fig. 2.7 with Figs. 2.2-2.4). Both the experimental and theoretical data show an initial relatively constant strain rate followed by a rapid decrease in strain rate as the strain approaches a limiting value. According to the viscous flow model the limiting value scales as the ratio of the grain boundary thickness to the grain size. The thickness of these films has recently been measured for a variety of compositions (Kleebe et al 1993a, 1993b). They are found to have a distinct value which depends on the composition and varies in a range from 0.5~2 nm. This yields strains of about 0.05%~0.2% if we assume the grain diameter is about 1μm and all the glassy films at grain boundaries under compression are squeezed out completely. This is in approximate agreement with the experimental value (Chadwick 1990).

Additionally, the viscous flow mechanism suggests an anelastic recovery on unloading. The redistribution of glass phase between grain boundary facets is only stabilized by an applied stress and there is a driving force to restore a uniform

glass film thickness once the stress is removed. Anelastic recovery has been observed following creep in silicon nitride (Arons et al 1980, Haig et al 1992).

Dissolution/reprecipitation has been proposed as one of the mechanisms responsible for steady-state creep (Lange et al 1980b, Kleebe et al 1994b). The constitutive equation for this process (Equ.2.3) predicts a linear relationship between the creep rate and the applied stress. Lange et al (1980b) studied the compressive creep of four compositions within Si_3N_4/MgO alloys, and found that two compositions with less glass phase exhibited no cavitation and had a stress exponent of n=1, suggesting the existence of the dissolution/reprecipitation mechanism. However, the other two compositions with more glass phase exhibited extensive cavitation and had a stress exponent of n=2, suggesting another mechanism, i.e. cavitation. Based on the observations, they concluded that both dissolution/reprecipitation and cavitation mechanisms exist during steady-state creep of silicon nitride. A shift from one mechanism to another depends on the additive composition. Most recently, Luecke and Wiederhorn (1994) analysed extensively the 1430°C creep of NT154, a commercial grade of silicon nitride doped with Y_2O_3, and found a significant difference between compressive creep and tensile creep of this material. In compression, this material creeps at a much lower rate than that in tension and the stress exponent is unity. In tension,

however, the creep rate is 10~100 times faster than in compression, and the stress exponent rises to 4. Furthermore, density measurements indicate cavitation contributes negligibly to the strain in compression, whereas in tension cavitation can account for 70~85% of the creep strain. Cavity morphology observed at the two-grain boundaries suggests that cavity growth occurs by a diffusive process as predicted by theoretical models. The material diffuses from the cavity surface to the grain surface within two-grain channels and results in cavities larger in size than the original grain boundary thickness. Clearly, the creep behaviour in compression of NT154 suggests a solution-reprecipitation mechanism, whereas cavitation leads to tensile creep. In the latter case, the total creep strain scales linearly with the volume fraction of cavities produced in creep.

Wilkinson (1994) recently gave a comprehensive explanation of the different creep responses exhibited in silicon nitride. For the mixed behaviour of exhaustion creep and steady-state creep (as shown in Fig. 2.2), he suggests that the initial creep period is controlled by viscous flow of the intergranular glass phase, until this process is exhausted by grain impingement. The creep rate then decreases and another mechanism appears following the viscous flow process. This suggests that the activation energy for viscous flow is smaller than that for steady-state mechanisms. According to his explanation, the temperature is very important in

determining the creep response of silicon nitride. At lower temperatures the steady-state creep rate is too low and only viscous flow creep is seen, exhibiting an exhaustion creep. At higher temperatures, the viscosity of the grain-boundary glass phase is too low, and thus viscous flow process is exhausted so quickly that it is incorporated into the initial loading transients, and only steady-state creep can be seen.

2.5 Effect of Oxidation and Crystallization on Creep Behaviour

The high temperature properties of glass-containing ceramics are limited or degraded by the intergranular glass phase because the glass begins to soften at relatively low temperature (about 1000°C). Changing the glass composition will have an influence on the high temperature properties. Therefore, the effect of oxidation and partial crystallization of the amorphous phase on creep behaviour should not be neglected, especially when these processes occur on the same time scale as the creep tests.

The crystallization of the amorphous secondary phase have been investigated in several systems. Lee et al (1988) studied a Si_3N_4 fabricated with a Y_2O_3 sintering aid and found crystallized $Y_2Si_2O_7$ at the grain boundaries. Wild et al (1972) found some evidence for the presence of $MgSiO_3$ in the grain-boundary phase of Mg-

containing silicon nitride. The most successful grain-boundary crystallization occured in the yttrium SiAlON system where yttrium aluminum garnet could be crystallized (Hohnke et al 1983, Lewis et al 1980). It is suggested (Lewis et al 1980) that the reduction in glass phase content accompanying the crystallization is associated with an improved creep resistance. Wiederhorn et al (1986) found that partial devitrification of a vitreous-bonded aluminum oxide could lower the strain rates and elongate failure times. Moreover, crystallization of secondary phases may change the chemical composition of the residual glass. If the impurities are not incorporated into crystalline secondary phases formed upon heat treatment, the impurities will be extruded to the residual glass. Kleebe et al (1994b) studied Yb_2O_3/Al_2O_3-fluxed Si_3N_4 with small additions of CaO and revealed the presence of a $Yb_2Si_2O_7$ crystalline phase. The Ca was found to segregate to the grain boundaries and increase substantially the grain-boundary film thickness, resulting in a degradation of creep resistance.

Oxidation can also change the composition of the sintering glass. During oxidation, the presence of amorphous grain-boundary phases provides a path for the outward diffusion of additive cations, nitrogen and impurity cations, and the inward diffusion of oxygen (Cinibulk and Kleebe 1993). Therefore, oxidation can purify the chemistry of the intergranular glass film and shift it to a lower M/Si ratio,

thereby increasing the refractoriness of the grain-boundary phase. Lange et al (1980b) studied the compressive creep behaviour of MgO doped Si_3N_4 materials and found that the truly steady-state creep does not exist during the creep process. The creep rate was always observed to slowly decrease with time. They ascribed this phenomenon to the effect of oxidation. Further work by the same investigators (Lange et al 1980c) shows that oxidation causes compositional changes and thus the creep mechanisms of the same materials shift from cavitational creep in the as-fabricated state to diffusional creep after oxidation.

From the above discussion, the creep properties of vitreous-bonded ceramics may change as the intergranular phase devitrifies or the materials are oxidized. Therefore, when microstruture development is correlated with resulting creep behaviour, crystallization or oxidation has to be considered.

CHAPTER 3

EXPERIMENTAL PROCEDURES

The objectives of this study included the examination of the effect of composition on creep mechanisms and the direct measurements of the redistribution of the intergranular phase after cerep. These goals were achieved by creep testing, TEM observations of the microstructural evolution during creep, density measurements and intergranular-film thickness measurements before and after creep. The experimental procedures are presented in this chapter.

3.1 Materials

Two different materials were used in this study ; a undoped silicon nitride and 800 wt. ppm Ba doped silicon nitride. The materials for this study were provided by H.-J. Kleebe of Universitat of Bayreuth, Germany. These materials were prepared from high purity Si_3N_4 powder, hot-pressed at 1925°C for 1h and 0.5h, respectively. The amount of additive and impurities were determined through X-ray fluoresence (XRF) analysis. The impurities such as Al, Ca, Fe, K, Na are all below 50 ppm (detectability of the current XRF analysis). Assuming the Ba was added in its oxide form, the Ba doped material had been sintered with 0.13 wt %

BaO, which is close to the nominal composition of 800 wt. ppm of Ba.

In this study, the materials were prepared from high purity Si_3N_4 powder. The purpose was to minimize the amounts of minor impurities. As we know, the properties of the intergranular glass phase are determined by its composition. However, most silicon nitride materials contain at least 4 or 5 elements such as Si, N, O and sintering aids. Impurities such as Ca, Fe, Al are also present in silicon nitride in the order of 100 ppm. Even this level of impurities is often sufficient to change the properties of material significantly when they are localized in the intergranular glass phase. So special attention has to be paid to the starting powder and sample preparation in order to have a clear understanding of the relationship between the creep behaviour and composition of the intergranular glass phase.

The BaO/Si_3N_4 system was used in the present investigation. There are several reasons to choose Ba as the dopant. First, Ba doped Si_3N_4 is a new grade of material which has never been investigated before. It has been found that Ca is a grain-boundary segregant in Si_3N_4 based materials, and can change the creep properties. Ba, having a similar chemistry to Ca, is expected to have a similar function. Thus the composition of silicon nitride grains will not be affected and all the dopant is used to change the composition of the intergranular glass phase.

Furthermore, the general microstructure will not be influenced by a small amount of dopant (800 wt. ppm), and thus quantititive comparison between materials with and without the dopant become possible.

If, following earlier studies (Tanaka et al 1994b), it is assumed that the undoped high purity Si_3N_4 material has 2.5 wt% SiO_2 as the only intergranular phase, then the Ba doped material contains both SiO_2 and BaO in the grain-boundary phase. The Ba concentration at the grain junctions in the 800 ppm doped material is estimated to be 3.6 wt% BaO/(BaO+SiO_2) on the assumption that all the Ba atoms in the 800 ppm doped material are localized in the glass phase which occupies about 3.0 vol.% of the material. According to the phase diagram (Fig.3.1), at temperatures below about 1370°C, the stable crystalline phases would be $BaO.2SiO_2$ and SiO_2.

SEM(scanning electron microscopy) was used to examine the microstructure of both materials in the as-sintered condition. To obtain good representations of grain size and grain aspect ratios, specimens were polished and then etched in 49% HF for 24 h to dissolve the grain-boundary phase, thereby revealing the grain morphology. Prior to examination, the etched specimens were gold-coated to prevent static charging in the SEM. Representative views of the morphology of the

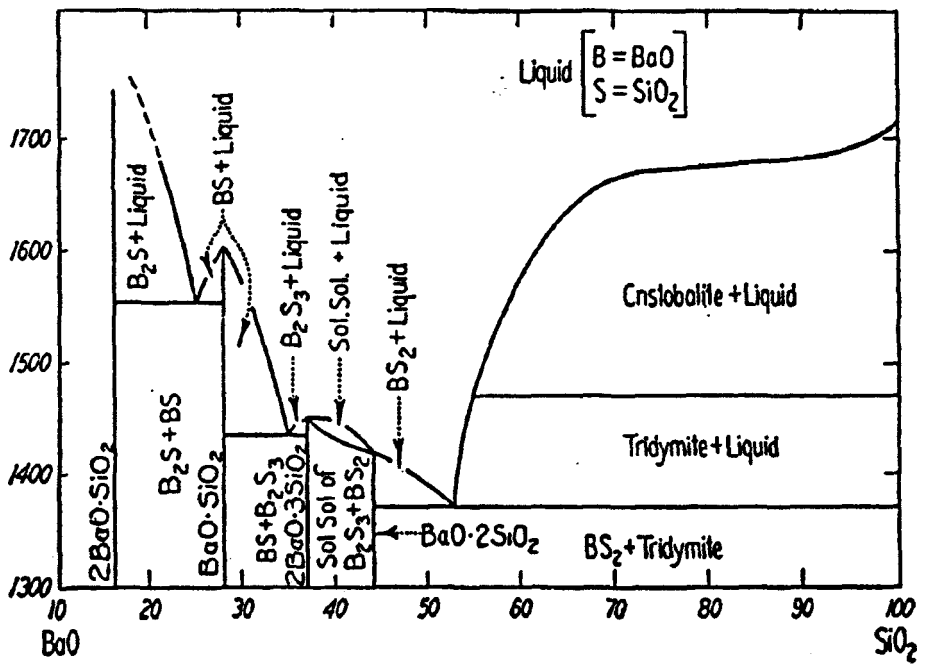

Fig.3.1 Phase diagram of $BaO\text{-}SiO_2$ (from Phase Diagrams for Ceramists. Edited by Reser M.K., The American Ceramic Society, Columbus, OH, 1964)

grain structure of the as-received materials are shown in Figs. 3.2(a) and (b). Figure 3.2(a) is an SEM micrograph of the undoped material, and figure 3.2(b) is an SEM micrograph of the Ba doped material. The SEM observations have shown that both materials contained equiaxed hexagonal β-Si_3N_4 grains, ranging in size from 0.2 to 0.3 μm, with more elongated grains 0.7 to 1.5 μm in length. The densities of the undoped and Ba doped materials used for this study were about 87% and 86% of the theoretical density of Si_3N_4, respectively.

3.2 Creep Experiments

Compression creep testing was used in the present investigation. Samples of about 2mm x 5mm x 7mm in size were diamond cut and ground at all surfaces. Special attention was paid to ensure the parallelism of the two end surfaces. The testing machine was a resistance-heated furnace with a loading jig using the lever arm principle. The push-rod and loading platens in contact with the sample were made from Al_2O_3 and SiC, respectively. The sample and platens were located in the centre of the furnace. Strain was measured using three direct-contact extensometers, with the two outer extensometers attached to the top platen, and the inner extensometer to the bottom platen. The motion of the platens were sensed by linear variable differential transducers (LVDTs). The output signals including

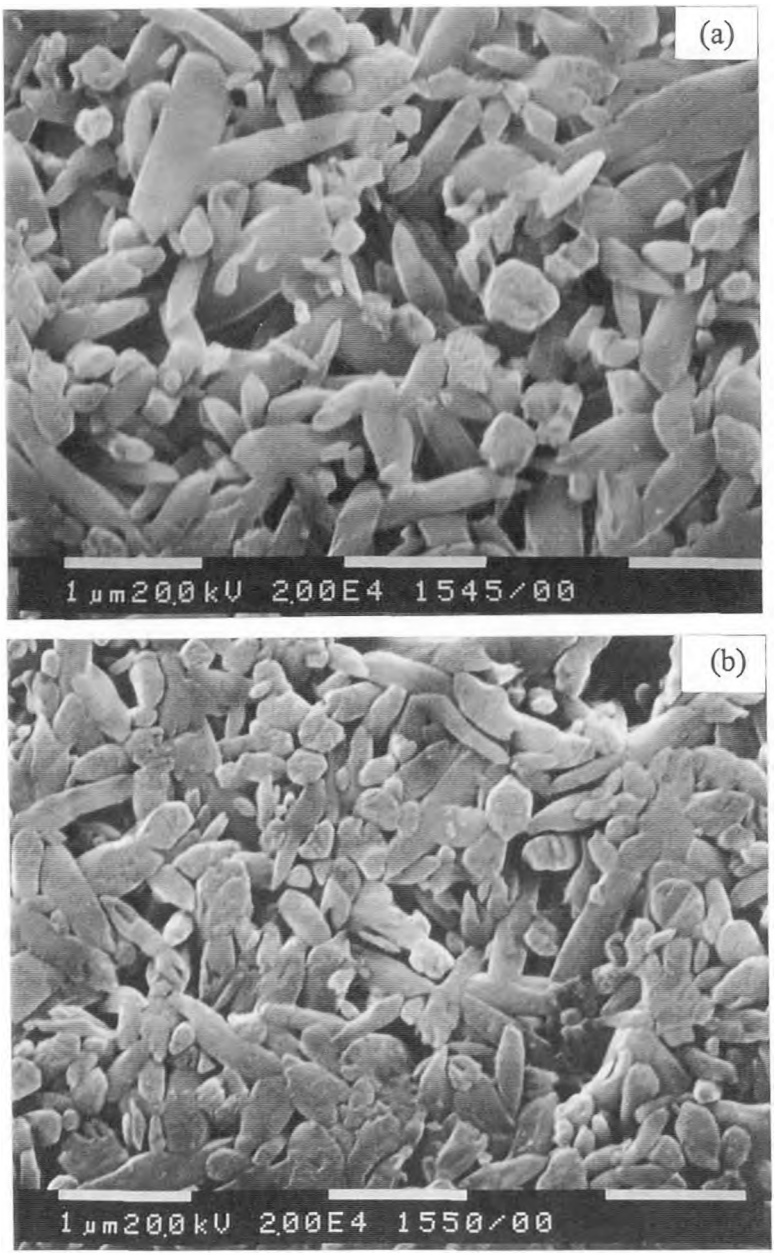

Fig. 3.2 SEM microstructure for the as-sintered silicon nitride materials (a) undoped, (b) 800ppm Ba doped, showing the equiaxed and elongated Si_3N_4 grains.

test temperature, sample displacement, strain and time were monitored and recorded by a PC. A schematic diagram of the loading configuration for compressive creep measurements is illustrated in Fig.3.3.

Tests were performed in air at stresses of 50, 100 and 200MPa at 1400°C. In order to minimize the effect of oxidation on the creep behaviour, a new sample was used at each stress level. Due to limited material, only one sample was tested at each experimental condition. To aviod strain recovery during cooling, the compressive load was not removed until the sample reached room temperature.

3.3 TEM Observation

The thin foils used for TEM observations were prepared by slicing the sample parallel to the stress axis into 500μm thick pieces using a diamond saw, grinding the material to a thickness of about 120μm using SiC paper, cutting 3mm discs with an ultrasonic drill and dimpling to about 20μm. The final thinning was by argon ion milling to perforation. The foils were subsequently carbon-coated to prevent electrostatic charging under the electron beam. TEM observations were performed in a Philips CM12 transmission electron microscope (accelerating voltage:120 keV), equipped with an EDAX analysis system.

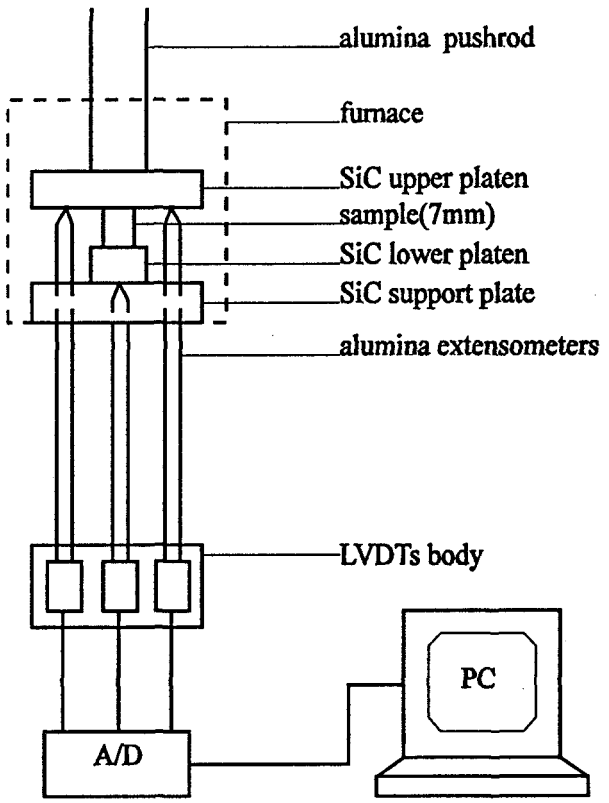

Fig. 3.3 Schematic diagram of loading configuration for compressive creep

3.4 Density Determination

The experimental materials contained about 13% and 14% by volume porosity, which might be expected to play a role during creep. Additionally, cavitation or cracking is also a possible mechanism for steady-state creep (Lange et al 1980b). Both of these can cause density changes. Thus, precise density measurements were necessary before and after creep. To avoid the possible closure of cavities and strain recovery caused by viscous flow of the intergranular glass phase during cooling, the compressive load was not removed until the sample was cool.

A water-displacement technique was used to measure the change in density. This method is accurate, easy to perform and nondestructive (Pennings et al 1989). First the weight, W_1, of the dry sample was measured in air to find the true mass of the sample. Then the sample was submerged into distilled water and the weight, W_2, of the sample in water was obtained. Finally, the third weight , W_3, of the wet sample in air was used to correct for the amount of water which has impregnated into the pores of the sample. The density , ρ, of the sample can be calculated from

$$\rho=\rho_{water}\frac{W_1}{W_3-W_2} \qquad (3.1)$$

where ρ_{water} is the density of distilled water (see details in the Appendix). Using this technique, the density of a specimen can be measured to an accuracy of ± 0.005 g/cm^3 , or within an error of $\pm 0.15\%$ in each density measurement. For crept specimens, 0.2 mm of the surfaces were ground off prior to measuring their densities, correcting for the possible density change caused by surface oxidation.

3.5 Film Thickness Measurements

The thickness of amorphous films at grain boundaries was measured by statistical analysis. Both the Fresnel fringe imaging (FFI) and the high-resolution imaging (HREM) techniques were used to image the intergranular glass films, as shown in Fig. 4.5. The principle of HREM technique is that for both adjacent grains interference fringes are produced on either side of the film. The thickness of the intergranular film is assumed to correspond to the area of discontinuity in these fringes at the interface. The FFI technique is based on the measurements of dark and bright fringes originating along the boundary, which is due to the discontinuity in the mean inner potential of the matrix grains and the amorphous grain-boundary film (Clarke 1979, Ness et al 1986).

To undertake a statistical evaluation of the film thickness, 20 grain boundaries were selected randomly in a given material. A thickness data point was measured at three different locations at each grain boundary, thus giving 60 data points for

a given material. Using these data, the distributions of the film-thickness values were plotted as histograms. The mean value and standard deviation of the film thickness were then determined. The standard deviation σ was determined using the following equation:

$$\sigma=\sqrt{\frac{1}{n-1}\sum_{i=1}^{n}(X_i-X)^2} \tag{3.2}$$

where X_i is the ith thickness measurement, X is the mean thickness value, and n is the number of film thickness measurements. Herein a distinct value of film thickness is assumed in a given as-sintered Si_3N_4material, independent of the grain boundary misorientation (Kleebe et al 1993b).

CHAPTER 4

EXPERIMENTAL RESULTS

4.1 Creep Results

4.1.1 General Behaviour

The compressive creep behaviour of both materials is shown in Fig. 4.1. The strain-time curves exhibit a continuous decreasing creep rate. In order to emphasize the initial creep behaviour, the data are presented in Fig.4.2 in terms of the strain rate as a function of strain on a log-log plot. As can be seen, two plateaus of strain rate occur during the creep process. The initial creep rate does not vary significantly with strain for both materials. After a strain of about $2\sim4\times10^{-3}$, the strain rate decreases by about one order of magnitude, suggesting two distinct creep stages, i.e., first stage of creep and second stage of creep. The second stage is usually refered to as steady-state creep (Lange et al 1980b). However, true steady-state creep does not seem to occur for these materials in the present investigation. The term "second stage of creep " seems more reasonable than that of "steady-state creep". The creep rate of the second stage had to be defined in a somewhat arbitrary way (Lange et al 1980b). Usually, the steady-state

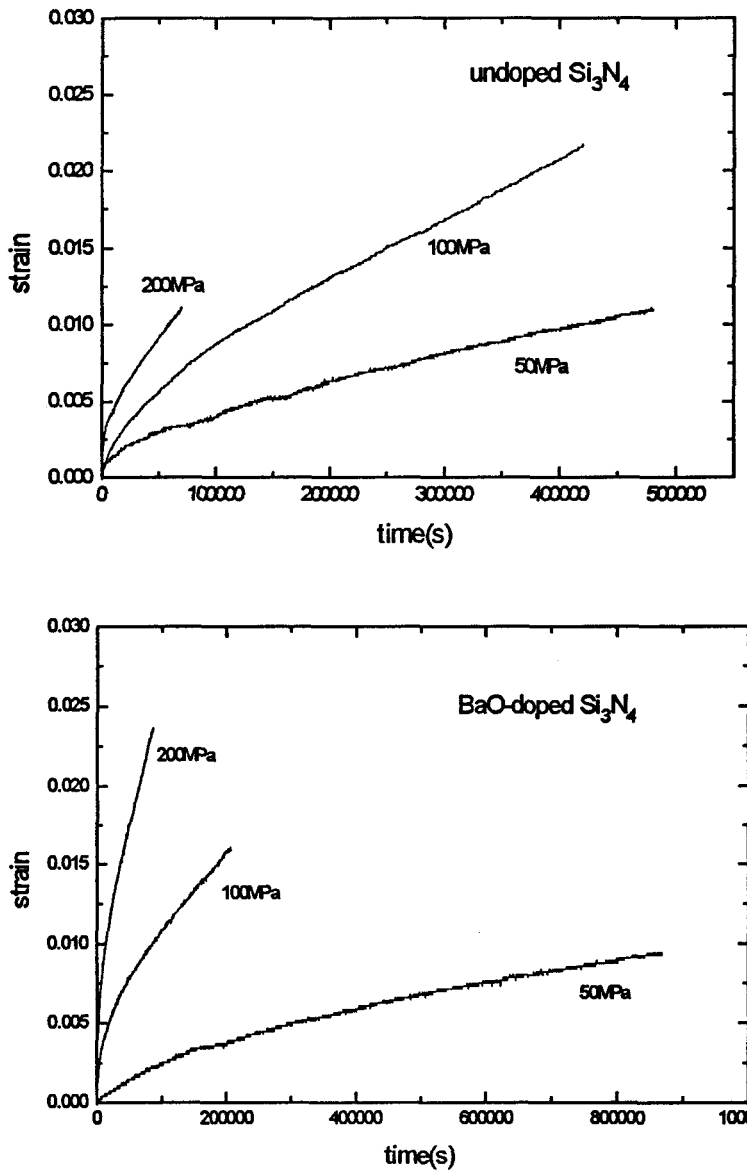

Fig. 4.1 Compression creep curves at 1400°C for the undoped and Ba doped silicon nitride materials under a variety of loads.

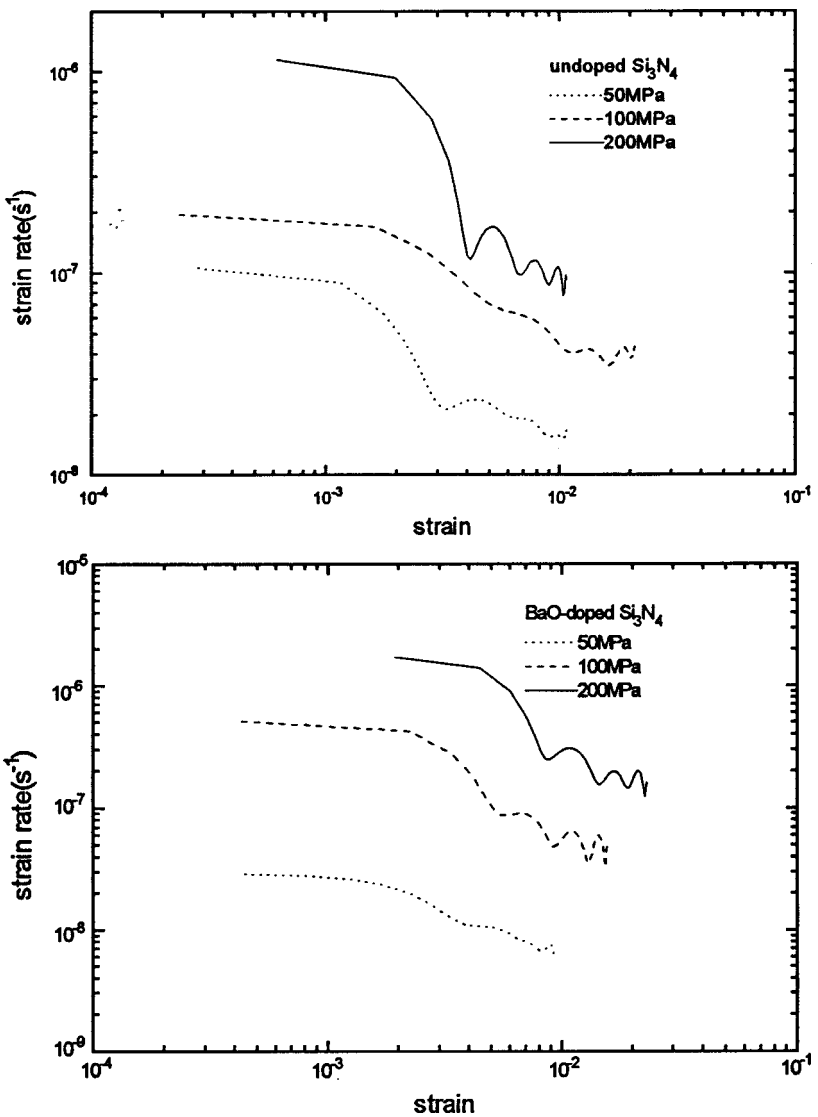

Fig.4.2 Creep resistance as a function of strain for silicon nitride materials with and without the Ba addition at 1400°C, corresponding to Fig.4.1.

creep rate ($\dot{\epsilon}$) is analysed with respect to the empirical Norton power-law relation

$$\dot{\varepsilon}=A\sigma^{n}e^{-Q/RT} \tag{4.1}$$

where A is a material constant, σ applied stress, n an exponent of applied stress, Q activation energy for creep, and RT is the product of the gas constant and absolute temperature. In order to characterize the Norton relation for these materials, the creep rate at 1% strain was taken as the steady-state creep rate. This assumes that the same strain corresponds to roughly equivalent microstructural changes in the different materials.

4.1.2 Stress Dependence of Creep Rate

The stress exponent n of the second stage of creep can be obtained from a log-log plot of strain rate vs. stress. The results are shown in Fig. 4.3(a). As can be seen, the undoped and Ba doped materials have different stress dependencies of the creep rate. The undoped material has a stress exponent of about 1, whereas the Ba doped material has a stress exponent of 2.6. The initial creep rate also obeys the Norton power-law relation, as shown in Fig.4.3(b). The stress exponent of the Ba doped Si_3N_4 is about 3.1, while the stress exponent of the undoped Si_3N_4 is about 1.7. These values suggest that the creep behaviour is determined by the composition of materials.

(a)

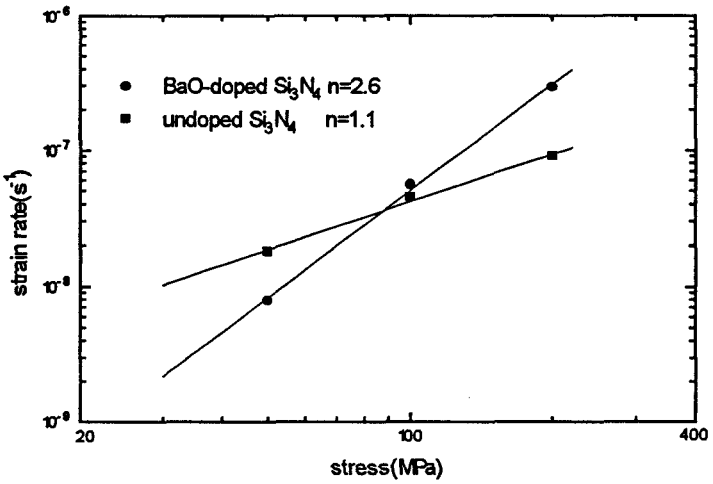

(b)

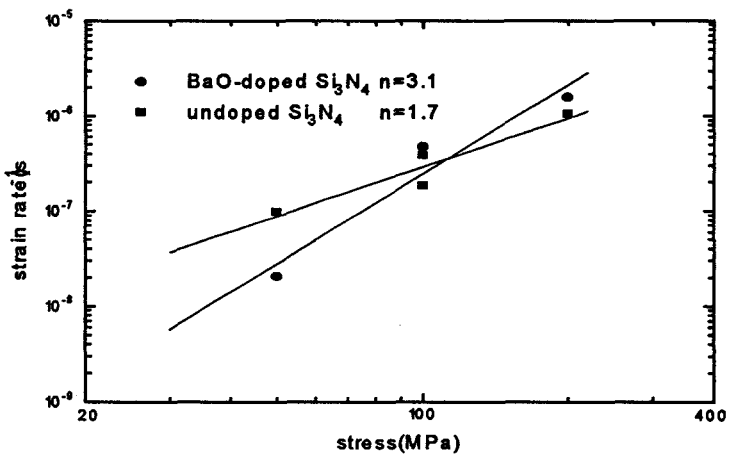

Fig.4.3 Stress dependence of the second stage creep rate (a), and the first stage creep rate (b) for the undoped and Ba doped silicon nitride at 1400°C.

4.2 Density Change

Precise density measurements were used to determine cavitation during creep. The results show that for the undoped material, there is almost no change in density of samples before and after creep, whereas densities of the crept samples of the Ba doped material decrease significantly compared with the as-sintered samples. The change in density when expressed as a volume fraction of cavities produced during creep for the Ba doped material as a function of creep strain is shown in Fig.4.4. It is assumed that the density change caused by oxidation was corrected when 0.2 mm was ground off the surfaces of crept samples (Chadwick 1990, Lange et al 1980b).

4.3 Microstructural Analysis

4.3.1 Intergranular Glass Phase

The microstructure of the experimental materials consisted of hexagonal and elongated β-Si_3N_4 grains (Fig. 3.2). TEM observations show that an amorphous phase exists both in the triple junctions as glass pockets and at two-grain boundaries as thin films (Fig.4.5(a)). Higher magnification of an amorphous film, with a width of about 1.4nm, in the Ba doped Si_3N_4, is shown in Fig. 4.5(b).

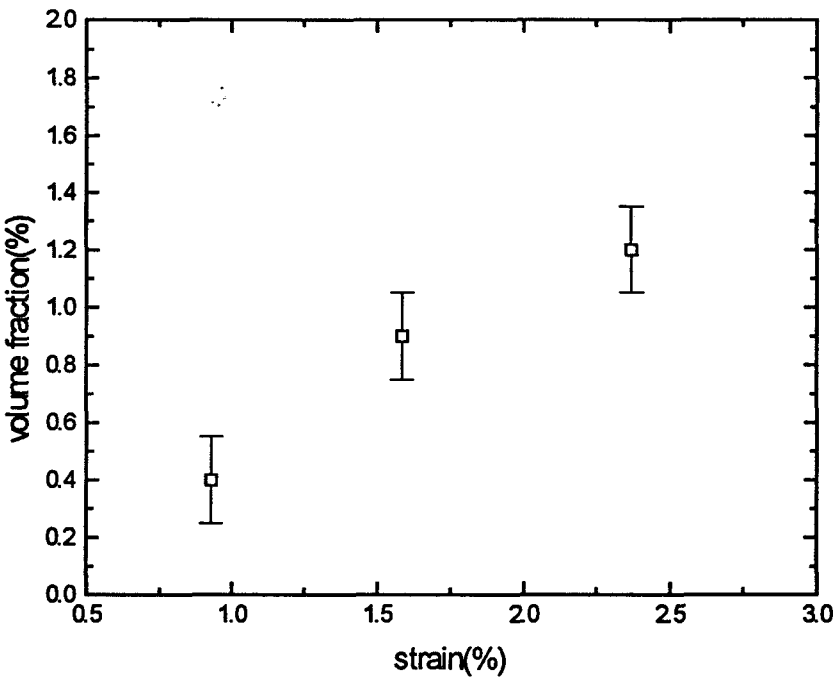

Fig.4.4 Volume fraction of cavities produced during creep as a function of strain in the Ba doped silicon nitride, tested at 1400°C under different stresses.

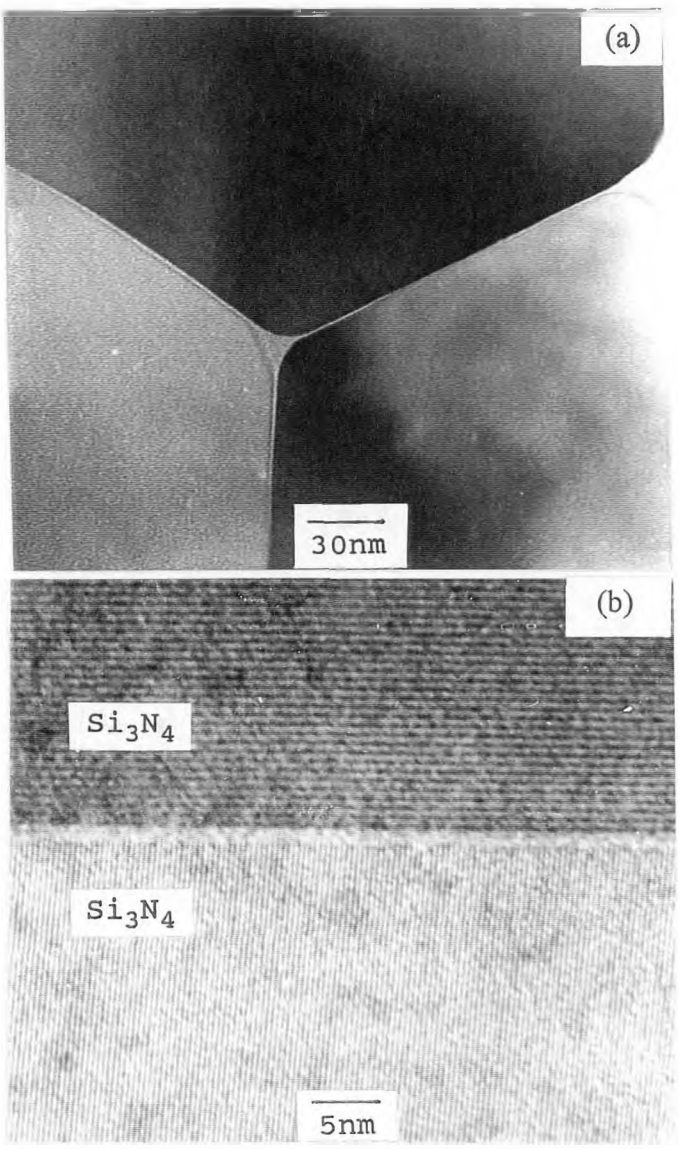

Fig. 4.5 (a) Bright-field image of an intergranular amorphous phase in the undoped silicon nitride (after creep at 1400°C,100MPa for 117h) observed by the Fresnel imaging technique; (b) High-resolution TEM image of an amorphous film(about 1.4nm thick) separated by two adjacent Si_3N_4 grains in the as-sintered Ba doped silicon nitride.

4.3.2 Cavities Produced by Creep

The result of density measurements suggests that cavitation or cracking must have occurred during creep of Ba doped material. This is verified by TEM observations. Since the as-received materials contained a high volume fraction of pre-existing cavities (about 13% and 14%), which existed at multi-grain junctions, and cavities can also be produced by ion-milling of TEM specimens, it is hard to distinguish the cavities produced during creep from the pre-existing cavities and those caused by ion-milling. Nevertheless, in the crept specimen of the Ba doped material, crack-like cavities were observed at two-grain boundaries, as shown in Fig.4.6. Such cavities were never observed in the as-sintered materials or in crept specimens of the undoped material under the same testing conditions. We believe these cavities were produced during creep and are not artifacts of sample preparation.

4.3.3 Strain Whorls at Grain Boundaries

In addition to observations of cavities at grain boundaries in the Ba doped Si_3N_4, strain whorls were also observed at grain boundaries of this material (Fig.4.7), whereas they were rarely seen in the undoped material (Fig.4.8), as indicated in Table 4.1.

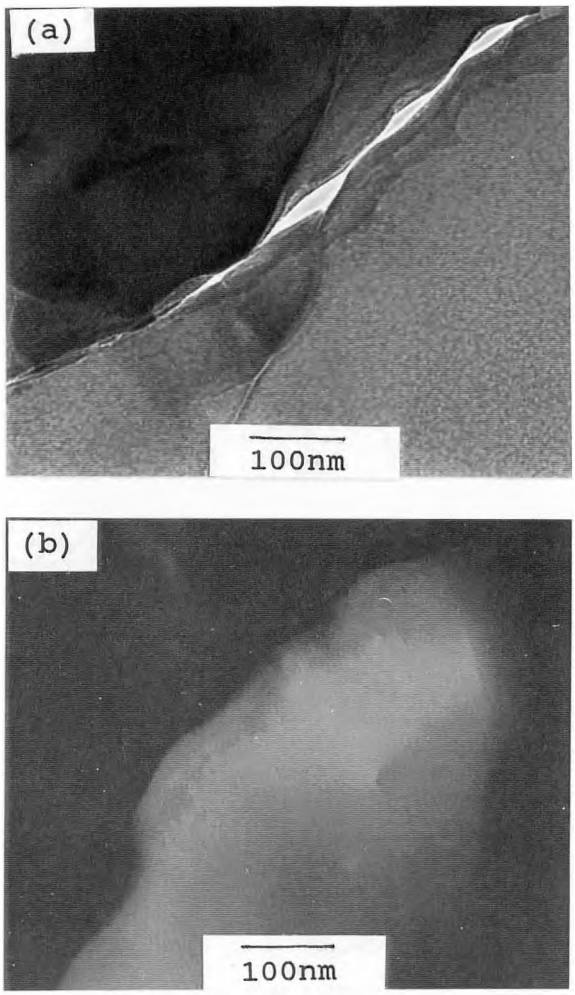

Fig.4.6 (a) Crack-like cavities which penetrated into the adjacent silicon nitride grains formed at two-grain boundaries in the Ba doped material after creep; (b) Dark-field image of the silicon nitride grain on the right indicating the cavities are intergranular.

The strain whorls were located only along two-grain boundaries and not seen at multi-grain junctions. When the foil specimen was tilted, the whorls changed their shape and orientations. Actually, these whorls are extinction contours resulting from a localized out-of-plane buckling of the TEM foil (Lange et al 1980b). Considering that there were no such features in the as-sintered materials, it is believed that the whorls are manifestations of a localized residual stress produced during creep.

Table 4.1 Occurrence of strain whorls

Materials	Undoped	Ba doped
As-sintered	Absent	Absent
Crept	Absent	Present

An interesting observation is shown in Fig.4.9. The high-resolution image of a strain whorl indicates clearly that the position of the strain whorl is exactly the contact site of two grains, where there is no glass phase.

TEM observations also indicate that there are steps or ledges on some grain boundaries, as shown in Fig.4.10. The ledge interference during creep may give rise to those strain whorls upon grain boundary sliding (Wiederhorn et al 1993, Lange et al 1980a).

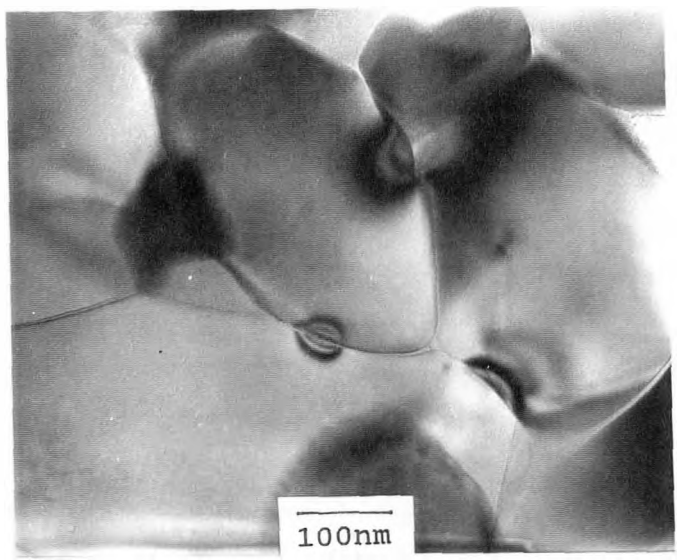

Fig. 4.7 Strain whorls produced at two-grain boundaries in the Ba doped material after creep at 1400°C, 200MPa for 24h.

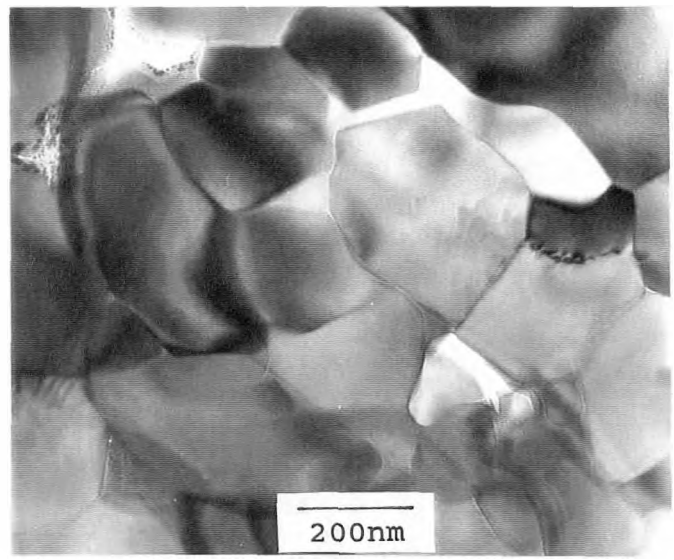

Fig.4.8 Typical microstructure of the undoped material after creep at 1400°C, 200MPa for 44h.

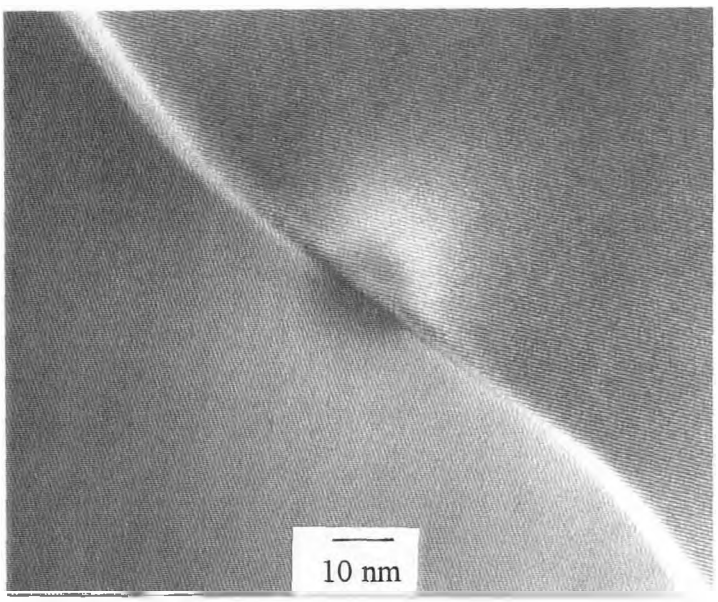

Fig.4.9 Higher magnification of a strain whorl in the Ba doped material after creep, indicating these strain whorls are manifestation of residual stresses due to grain-to-grain contact.

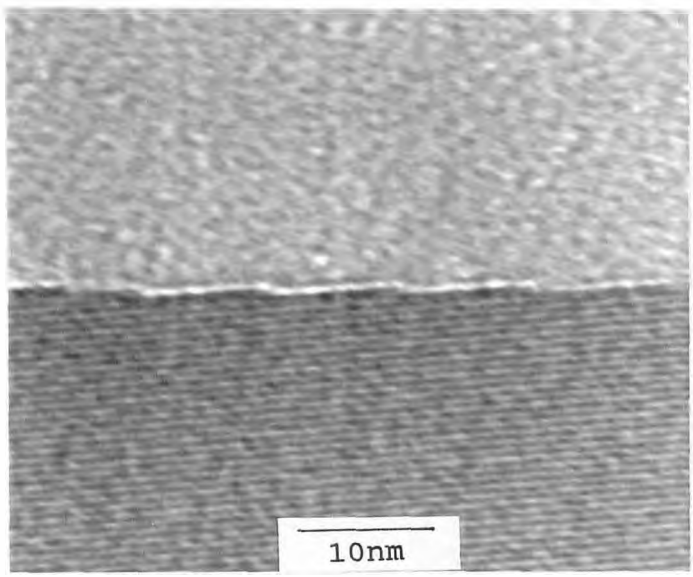

Fig.4.10 Bright-field image of a grain boundary with steps or ledges along it.

4.3.4 Redistribution of Intergranular Glass

Figures 4.11 and 4.12 present the measured values of grain-boundary film thickness in the undoped and Ba doped materials. As indicated in Table 4.2, the mean value of film thickness is 1.00±0.13 nm for the undoped Si_3N_4 and 1.41±0.15 nm for the Ba doped Si_3N_4 in their as-sintered conditions. These results suggest that the thickness of the intergranular film depends on material composition. After creep, the mean film thickness for both materials remains unchanged. However, the standard deviation of thickness measurements increased substantially, from 0.13 nm to 0.30 nm for the undoped material crept under a stress of 100MPa, and from 0.15 nm to 0.59 nm for the Ba doped material crept under a stress of 200MPa. This implies that the intergranular glass phase was redistributed after creep.

Table 4.2 Measured values of grain-boundary film thickness (nm)

Material	Undoped	Ba doped
As-sintered	1.00±0.13	1.41±0.15
Crept	1.05±0.30	1.40±0.59

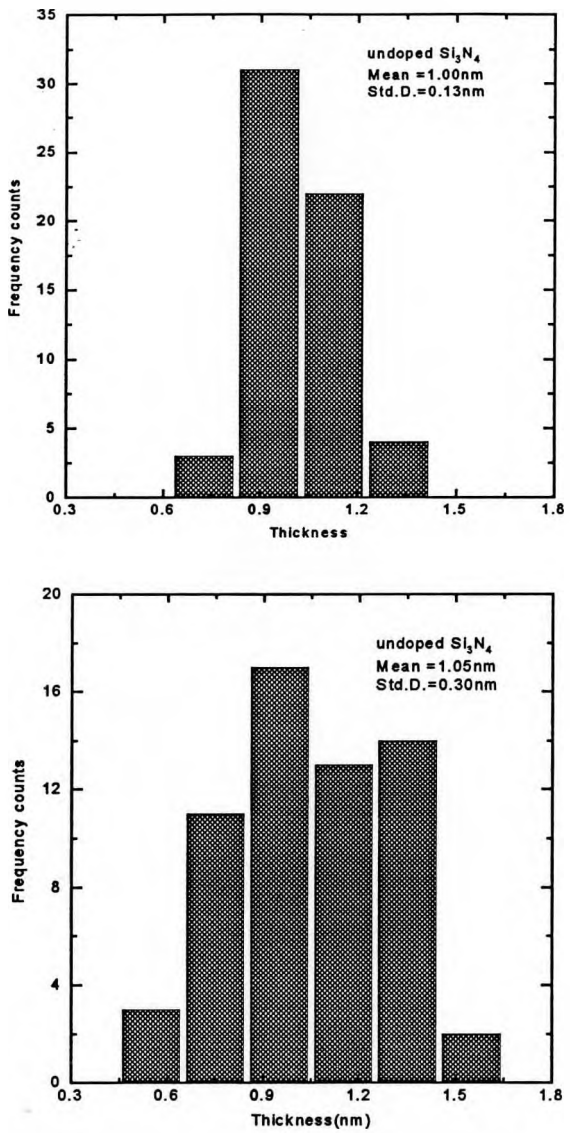

Fig.4.11 Histograms of the film thickness distributions of the undoped silicon nitride: (a) before creep; and (b) after creep at 1400°C for 117h under the load of 100MPa (total strain 2.2%).

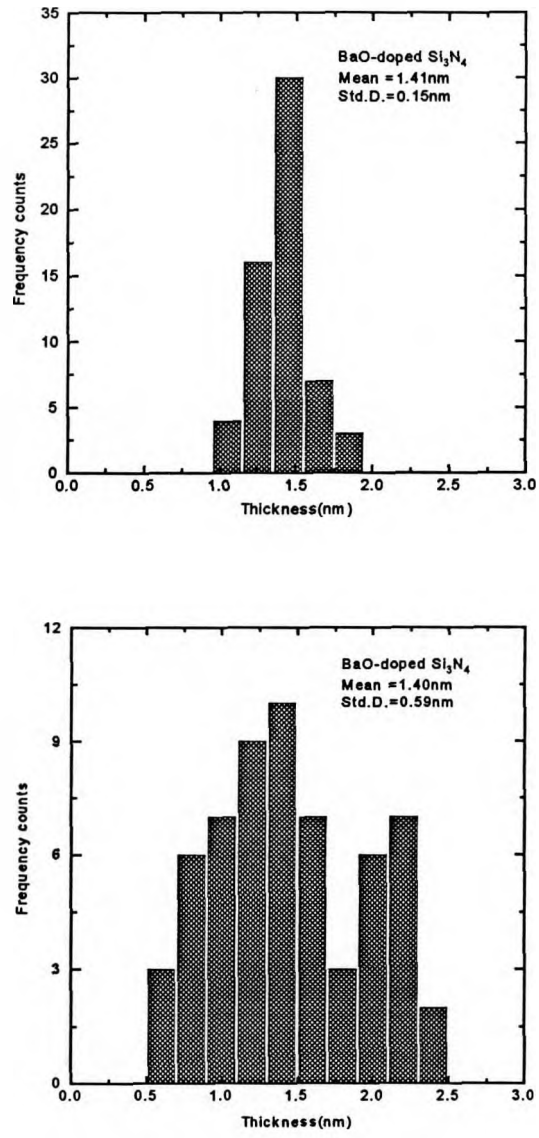

Fig.4.12 Histograms of the film thickness distributions of the Ba doped silicon nitride: (a) before creep, and (b) after creep at 1400°C for 24 h under the load of 200MPa (total strain 2.4%).

CHAPTER 5

DISCUSSION

In this chapter, the creep mechanisms of silicon nitride materials with different compositions of grain-boundary phase will be discussed based on the observed macroscopic creep behaviour and microstructural analysis. Some important phenomena or results such as work hardening during creep process and the influence of Ba addition on the grain boundary phase will also be discussed.

5.1 Creep Mechanisms

Both the undoped and Ba-doped Si_3N_4 materials exhibit a similar creep behaviour. In the first creep stage, the strain rate remains relatively constant and then decreases abruptly when the strain reaches a critical value after which the creep approaches an apparent steady-state regime (i.e., second creep stage) (Fig. 4.2). The one order of magnitude difference in strain rate between the two creep stages suggests that more than one creep mechanism operates. Based on the present investigation and the previous work of other investigators, we ascribe the viscous flow mechanism to the first stage of creep. The second stage of creep is dominated by either dissolution-reprecipitation or grain boundary sliding accommodated by

cavitation, depending on the composition of materials.

5.1.1 First Stage of Creep

(1) Comparison with the literature

The initial creep behaviour exhibited in the present study has also been observed by Chadwick and Wilkinson et al (1990, 1992, 1993). They studied the four-point bending and compression creep behaviour of Kyocera SN220, a commercial Si_3N_4 material doped with 4wt%Y_2O_3 and 4wt% Al_2O_3 and obtained similar results. "The steady state creep rate in SN220 is found at low strains (less than 0.3%). At higher strains the strain rate decreases continuously" (Chadwick 1990).

It should be noted that an initial constant strain rate regime has not generally been noted by other groups studying the creep of silicon nitride materials. This may be because very few previous studies have looked at strain rate data carefully at low strains. Another reason is that the viscosity of the intergranular phase is very low and creep due to viscous flow process occurs very fast. Based on this assumption, Wilkinson (1994) used the creep data of other groups and presented the creep rate as a function of strain on a log-log plot. The results are very encouraging. For example, the creep response of a HIPed Y_2O_3 doped Si_3N_4, NT154, exhibits two plateaus, the second plateau decreasing in strain rate by about one order of

magnitude (Fig.2.3). In the present investigation, the creep behaviour exhibited in the first creep stage is independent of the material composition in terms of the shape of creep curves.

(2) Viscous flow model applied to the first stage of creep

Such creep behaviour exhibited in the first stage, recently termed "exhaustion creep" (Wilkinson 1994), has been postulated as due to the viscous flow mechanism. However, the evidence for this process has been hitherto indirect only. In the present investigation, the statistical data for the change of grain-boundary thickness before and after creep (Figs.4.11 and 4.12) suggests a significant redistribution of the intergranular glass phase. This suggestion can be reasonably deduced from the change in the standard deviations of film thickness measurements. The standard deviations for the as-sintered materials are about 0.15nm, which is consistent with the obtainable accuracy of ±0.15nm using the Fresnel fringe imaging technique (Tanaka et al 1994a). This indicates that the as-sintered materials have distinct values of the film widths, independent of grain boundary misorientations. The larger standard deviations after creep can only be explained by a greater film thickness distribution. This implies that grain boundaries under compression become thinner while those under tension become thicker. The schematic diagram of the grain-boundary film thickness change before

and after creep is shown in Fig. 5.1. Although the precise change in the thickness of grain boundaries of approaching grains during compressive creep is still unknown, the redistribution of intergranular glass provides, for the first time, direct evidence for the viscous flow mechanism.

Applying the model of Dryden et al (1989, 1995) to the first creep stage, we can imagine such a deformation process of silicon nitride. Upon application of a load, the siliceous material lying on the grain boundaries under compression is squeezed out to the grain boundaries under tension. The separation between adjacent grains is changed to accommodate the intergranular glass redistribution. Evidently, as the separation between the adjacent grains under compression decreases, it becomes more and more difficult to expel the glass from between the grains. As a result, the creep rate exhibits a continuous decrease with strain during viscous flow process. When all of the fluid is squeezed out from between grain boundaries perpendicular to the compressive stress axis, the strain rate decreases drastically and creep by this mechanism stops. The maximum strain contributed by this process is on the order of the ratio of the intergranular film thickness to the grain diameter.

Using the constitutive equation (Equ. 2.2) developed by Dryden and Wilkinson (1995) for creep due to non-linear viscous flow, the creep resistance as a function

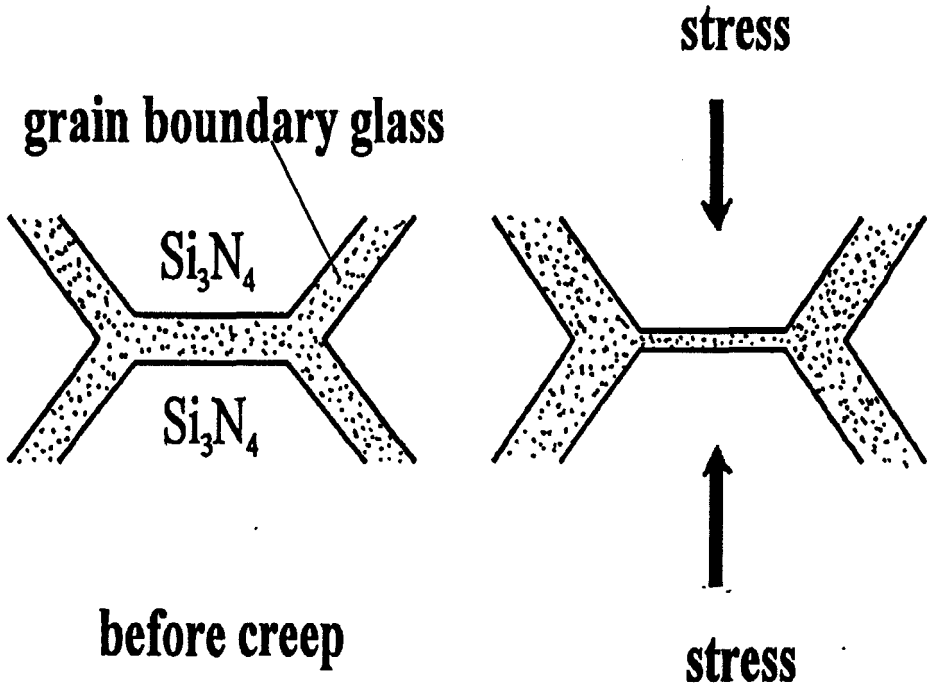

Fig. 5.1 Schematic diagram of the grain-boundary film thickness change before and after creep

of strain can be predicted theoretically. As shown in Fig.2.7, the creep rate is expected to decrease continuously with strain during viscous flow of the fluid and the creep stops when the grains contact. It is evident that the theoretical expectations are consistent with the present experimental results (Fig.4.2). However, experimental results show that after the maximum strain, creep continues at a much lower rate instead of stopping. This suggests that another mechanism becomes more important after the maximum strain, which will be discussed in the next section.

The model of equilibrium film thickness developed by Clarke (1987) provides additional support for the viscous flow mechanism. This model suggests that when a normal stress is applied to a grain boundary the film thickness will change until a new equilibrium is established. "This process requires the viscous flow of the amorphous phase and its redistribution according to the local normal stress on each grain boundary facet" (Wilkinson 1994). This model predicts that grain boundary glass phase would remain (with a reduced thickness) even under a compressive stress. With an increase in stress, the amount of glass squeezed from between the grain boundaries is expected to increase. Therefore, the strain at which the strain rate starts to decrease drastically would be predicted to increase with increasing applied compressive stress. This is consistent with the observed creep responses

under different levels of loads (as shown in Fig. 4.2). For example, in the Ba doped material, the strain at the end of the first plateau increases from $2x10^{-3}$ to $4x10^{-3}$ when the stress increases from 50 MPa to 200MPa.

If we consider the microstructure of the material to be composed of rigid hexagonal grains separated by viscous fluid, the maximum strain ϵ_{max} due to viscous flow can be estimated from these models as the ratio of the difference in the equilibrium grain-boundary film thickness before and after creep to the grain diameter. In the undoped Si_3N_4 material, it is assumed that only SiO_2 existed at the grain boundaries. Using Clarke's equilibrium thickness theory (Clarke 1987) and inserting the appropriate numerical values for the different parameters in his force balance equation, an equilibrium film thickness of 1.03nm is obtained. This value is very close to the measured results shown in Fig.4.11. From Fig.3.1, we know that both the undoped and Ba doped Si_3N_4 have an average grain size of 0.25μm for the equiaxed hexagonal grains. We assume that the film thickness change before and after creep is the difference in the standard deviation, i.e., 0.17nm for the undoped Si_3N_4 under the load of 100MPa and 0.44nm for the Ba doped Si_3N_4 under a load of 200MPa. From this the maximum strain in compression due to viscous flow can be estimated as about 0.1% and 0.2% for the two cases, respectively. These values are similar to the observed values of the

strain corresponding to the end of the first plateau in the strain rate vs strain curves (Fig.4.2), which are 0.2% for the undoped Si_3N_4 and 0.4% for the Ba doped Si_3N_4. It should be noted that the values of film thickness change used in the calculations are approximate. Given this reservation, the calculated values of the maximum strain by the viscous flow mechanism are in good agreement with the experimental results observed.

Chadwick and Wilkinson et al (1992, 1993) extended the model of Dryden et al (1989) to non-linear viscous fluids. In the present investigation, the stress exponents of both materials for the initial transient creep stage are 1.7 and 3.1, respectively (Fig.4.3(b)), which are larger than unity. This suggests the intergranular fluids are behaving in a non-Newtonian fashion. The different stress dependencies of the initial creep rate probably reflect the different properties of the SiO_2 glass phase in the undoped Si_3N_4 and $BaO\text{-}SiO_2$ glass phase in the Ba doped Si_3N_4 material.

5.1.2 Second Stage of Creep

(1) Comparison with the literature

The results of this study show that both the undoped and the Ba doped silicon

nitride exhibit a second creep stage following the exhaustion creep. However, the strain rate/stress exponents are different, suggesting that different mechanisms dominate the second stage of creep of the two materials. Additionally, the microstructural evolutions of the two materials during creep are also different. The Ba doped materials exhibited obvious cavitation at grain boundaries after creep, whereas there were no such features in the undoped material. This compositional dependence of creep behaviour has also been reported by other investigators (Lange et al 1980b, Tanaka et al 1995). Tanaka et al (1995) studied the high temperature creep of a low Ca-doped Si_3N_4 at 1400°C under four-point bending, and found that a 80 ppm Ca addition decreased the stress exponent to 1.0 whereas the stress exponent of undoped Si_3N_4 was 1.3. The lower stress exponent caused by Ca addition may be attributed to the observation that the thinnest intergranular films form at 80 ppm Ca (Tanaka et al 1994b). Lange et al (1980b) studied the compressive creep of four compositions of MgO-doped Si_3N_4 at 1400°C, and obtained very similar results to the present investigation. The two compositions with more intergranular glass exhibited extensive cavitation and had a stress exponent of about 2, indicating a cavitation mechanism, whereas the other two compositions with less glass phase exhibited very little cavitation and had a stress exponent of about 1, suggesting a diffusional creep process. Some investigators, however, seem to suggest that the stress state plays a more important role than the

composition of the material in determining the creep mechanisms. For instance, Luecke and Wiederhorn (1994) studied extensively the creep mechanisms of some silicon nitride ceramics and found that the stress exponent in tension is 3~5 while in compression the stress exponent is about 1. In this study, different values of stress exponent were observed in the compressive creep of the experimental materials. Based on the experimental results, the behaviour of the undoped material is ascribed to dissolution-reprecipitation and the Ba doped material is suggested to be dominated by grain boundary sliding accommodated by cavitation.

(2) Dissolution-reprecipitation model applied to the undoped material

In polycrystalline ceramics and metals, creep is attributed to dislocation motion, diffusional creep (Herring 1953, Coble 1963) and cavitation. It is generally accepted that dislocation creep does not operate in silicon nitride because there is no clear evidence that dislocations are generated or that they move at the creep temperatures (Kossowsky et al 1991, Lange et al 1980b and Wiederhorn et al 1994). For instance, Wiederhorn et al (1994) studied a number of grades of silicon nitride tested in tension and found no indication of dislocation generation. In a study of compressive creep of four grades of hot-pressed silicon nitride , Lange et al (1980b) reached the same conclusion. Although dislocations may be observed

in the silicon nitride grains, no evidence could be found for dislocation activity during creep from the microstructure before and after creep. In the present study, the experimental materials are almost free of dislocations before and after creep. Therefore, dislocation creep is not a dominant mechanism in the present investigation.

As we know, a stress exponent of unity is strong evidence for a diffusion controlled mechanism (Pharr et al 1983, Raj et al 1981 and Raj 1982). The lack of dislocation motion, a stress exponent of about 1 and no cavitation in the undoped silicon nitride suggest a diffusional mechanism. Creep occurs by dissolution of silicon nitride from grain boundaries in compression and reprecipitation on grain boundaries in tension, thereby changing the shape of grains. Although it is impossible in the present study to give direct evidence for a change in grain size and shape before and after creep because the strain (<2.5%) is too small, the existence of lens-shaped cavities at grain boundaries (Fig. 4.6) confirms that silicon nitride can diffuse through the intergranular glass phase at 1400°C. Lens-shaped cavities usually grow by a Hull-Rimmer type process (1959), which requires diffusion along the surfaces of cavities into and along the grain boundary. The glass phase at grain boundaries provides a fast transport path which favours

Coble creep (Coble 1963) over Nabarro-Herring creep (Herring 1950, Nabarro 1948). It is therefore reasonable to attribute the deformation process to Coble creep. Fig. 5.2 illustrates schematically the process of dissolution-reprecipitation creep. The same conclusion has also been reached by Lange et al (1980b) and Wiederhorn et al (1994) in their studies of different materials.

(3) Cavitation model applied to the Ba doped material

With regard to the Ba doped material, we ascribe the second stage of creep to grain boundary sliding accommodated by cavitation. This conclusion can be reasonably reached by the experimental observations. First, the stress exponent of about 2 rules out the possibility of simple diffusional creep. Dislocation motion is not a dominant mechanism of creep deformation. Secondly, the density decrease of the crept specimens, combined with the direct TEM observations of cavities or cracks at grain boundaries, suggests that creep occurs by a cavity-related process. A large number of strain whorls at grain boundaries due to grain-to-grain contact indicates that the growth of cavities is caused by grain boundary sliding.

The strain whorls in the crept specimens have also been observed by other investigators (Lange et al 1980a, Wiederhorn et al 1993). In general, these strain

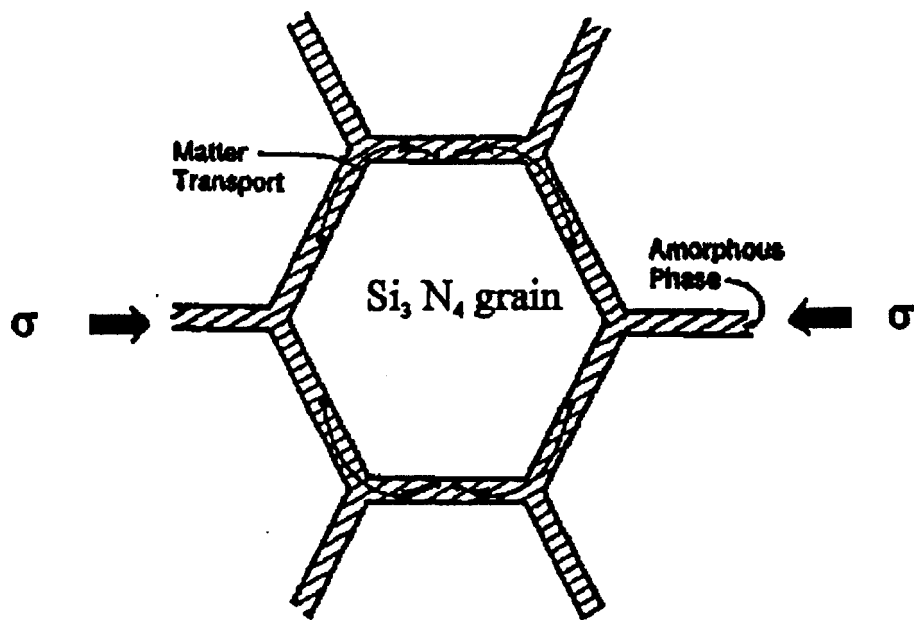

Fig. 5.2 Schematic illustration of the process of dissolution-reprecipitation creep

whorls have been considered as evidence of grain boundary sliding. As pointed out by Wiederhorn et al (1993), the grain boundaries in the silicon nitride are not flat and smooth (Figs. 4.9 and 4.10), and they will become interlocked as grain boundary sliding occurs. Contact can be made either at curved surfaces (Fig.4.9) or at asperities on grain boundaries, which hinders sliding and results in strain whorls. In the latter case, it is suggested by Lange et al (1980a) that the size of these asperities must be roughly equal to the thickness of the grain-boundary phase (i.e. about 1 ~ 2 nm), and that the most probable sources of these asperities are ledges of single and multiple interplanar height at grain boundaries. However, within the resolution of their TEM studies, Lange et al. did not find these small ledges. In the present work, however, ledges composed of one or more lattice planes have been found along two-grain boundaries. It is likely that asperities of opposing sign lock together during sliding, which results in the observed strain whorls. Fig. 5.3 illustrates schematically how strain whorls are produced during grain boundary sliding.

Cavities are also observed on grain boundaries of the Ba doped material. The following is our explanation for cavitation. As grain boundary sliding proceeds, the creep resistance is produced by the development of contact between grains. When the local resistance of creep becomes large enough, sliding will cease and

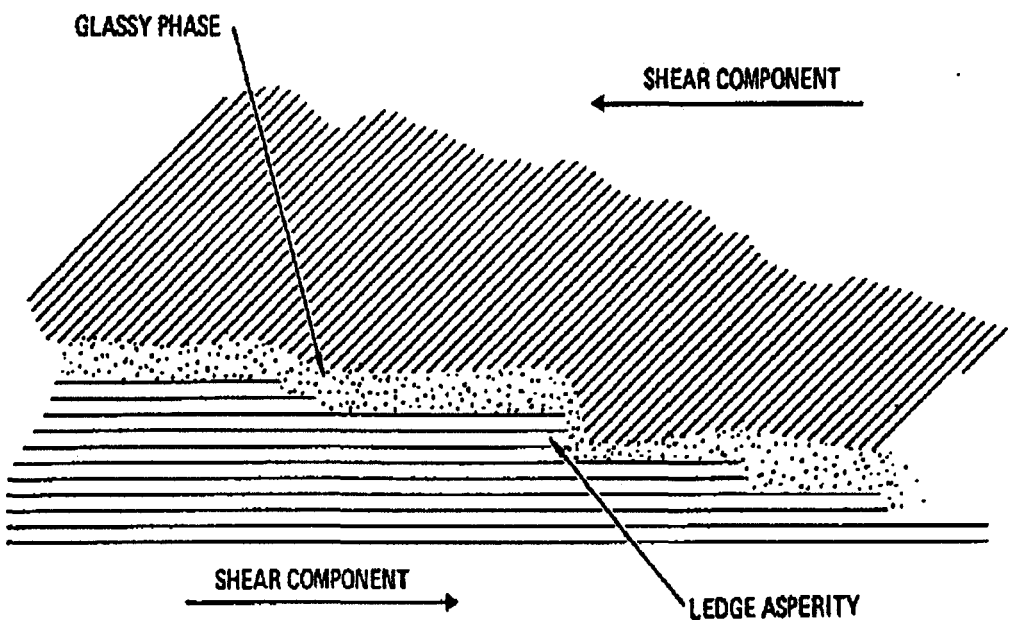

Fig. 5.3 Model of grain boundary sliding which gives rise to strain whorls (Lange et al 1980a).

cavitation will occur. Cavitation, as a stress release mechanism, occurs at the most highly stressed area. When the stress is relaxed, grain boundary sliding continues and then causes a highly stressed area in other locations. This viewpoint was also recently proposed by Wiederhorn et al (1993). In fact, according to Wiederhorn et al (1993), "the role of grain boundary steps or curved surfaces in impeding grain boundary sliding and in nucleating cavities is widely accepted in material literature". Evidently, the rate of grain boundary sliding will determine the rate at which cavitation occurs. Furthermore, if the rate of cavity nucleation and growth is very fast, the creep rate is also controlled by the rate of sliding of the grain boundaries.

From the above discussion, we can conclude that the lens-shaped cavities observed at grain boundaries are produced by grain boundary sliding. According to Tsai and Raj (1982), grain boundary sliding can also produce cavities in the triple junctions. They proposed that the dense packing of silicon nitride grains required an expansion in volume for the particles to move past one another. Dilation results in a negative pressure within the silicate phase, which is sufficient to nucleate cavities during deformation. Therefore, some of the cavities at triple junctions observed in the crept specimens of the Ba doped material are believed to be produced by grain boundary sliding during creep deformation. According to the density measurements

(Fig.4.4), the cavities produced during creep account for about 55% of the total creep strain. This result is very similar to that reported by Lange et al (1980b) in their study of the compressive creep of MgO doped silicon nitride materials.

It should be noted that the role of the pre-existing cavities is not very clear. A compressive load is likely to result in a reduction in the size of the pre-existing cavities, thus increasing the density of the crept specimen. However, this was not observed in the present study. The density of the undoped material was not changed, or changed within the accuracy of the density measurements (±0.15%), before and after creep, which suggests that the pre-existing cavities play a minor role in creep in the present study.

5.1.3 Summary

In this section, the creep mechanisms of the experimental materials during different stages have been discussed. The results are shown schematically in Fig. 5.4. One can imagine such a creep scenario for compressive deformation of silicon nitride. Once a load is applied, silicon nitride grains are displaced in such a way that excess amorphous phase at compressive grain boundaries is squeezed out from between the grains. This viscous flow deformation ceases when a new equilibrium thickness is reached (Wilkinson 1994). However, this is soon replaced by the

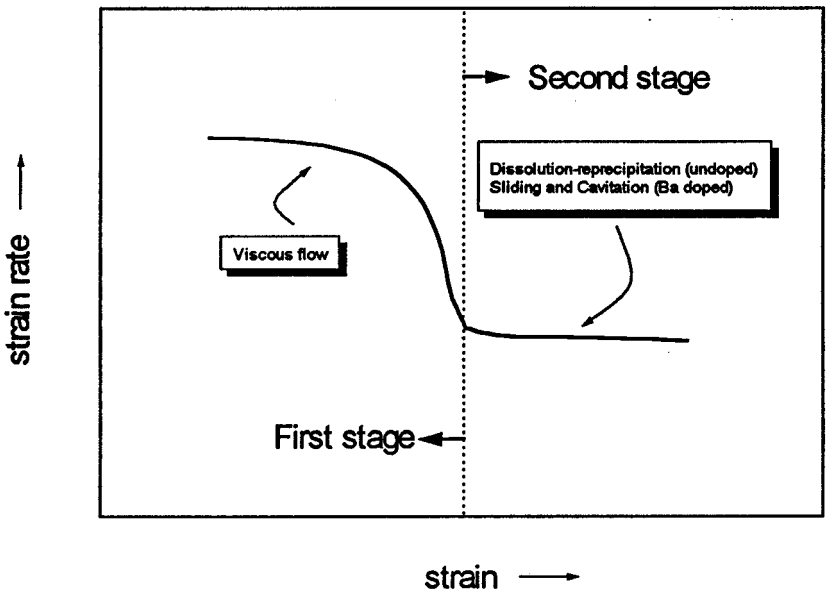

Fig. 5.4 Schematic diagram of creep mechanisms during different creep stages

appearance of a new mechanism, which is determined by the properties of the secondary glass phase. For the undoped material, the activation energy for dissolution-reprecipitation is smaller than cavitation, so diffusional creep occurs during the second creep stage. For the Ba doped material, the grains slide over one another after viscous flow. This mode of deformation is restricted by the grain contact and/or the development of a negative pressure within the triple silicate phase. If the silicate phase does not cavitate, then sliding will cease. If cavitation occurs, the deformation by sliding will continue. The creep rate contributed by viscous flow is much higher than that by either of the second stage mechanisms. So the creep response exhibited in the curves of strain rate vs strain is the occurrence of two plateaus.

5.2 Work Hardening Phenomenon

An important characteristic of the creep behaviour of the experimental materials used in the present study is the occurrence of a decreasing strain rate with time for all conditions of testing, not only in the intial creep (first stage of creep) but also in the apparent steady-state creep regime (second stage of creep). This phenomenon has also been observed by other investigators (Lange et al 1980b, Gurther et al 1990, Hockey et al 1991). In other studies, this work hardening has

been attributed to a gradual increase in refractoriness of the intergranular phase caused by the diffusion of impurities and cations from the intergranular glass to the surface oxide layer and of oxygen from the surface into the bulk. In a recent study by Wiederhorn et al (1993) on the tensile creep of a HIPed silicon nitride containing 4wt% Y_2O_3 as a sintering aid, transient creep was found to last for prolonged periods (i.e., over 1000h). Based on the observation of strain whorls at grain boundaries, they proposed that the transient creep was primarily a consequence of intergranular contact as the grains of silicon nitride slid over one another.

In the present study, the time-dependent strain rate in the first stage of creep has been explained by a viscous flow mechanism. In the second stage of creep, two mechanisms were introduced to explain the different creep behaviours exhibited in the different materials, i.e., dissolution-reprecipitation and grain boundary sliding. The dissolution-reprecipitation mechanism is expected to give rise to steady-state creep. Thus, the work hardening phenomenon has to be explained. Models of grain boundary sliding are also usually based on assumptions that lead to steady-state creep, so some modifications of these models is required to explain the transient creep behaviour. It should be noted that devitrification of intergranular phase is not a possible explanation of work hardening because no

secondary crystalline phases were observed at grain boundaries in the crept specimens of either material.

In the undoped material, neither cavitation nor strain whorls were observed at grain boundaries. It is suggested that the creep resistance of this material is improved by oxidation. In the dissolution-reprecipitation process, intergranular glass provides a path of high diffusivity . The strain rate is related to the viscosity of the intergranular glass. The constitutive equation for this process, whose kinetics is controlled by diffusion through the glass phase , is given by equation 2.3. An increase in the refractoriness of glass will result in a decrease in strain rate.

In the Ba doped material, work hardening can be attributed to the effects of oxidation and intergranular contact due to grain boundary sliding. Many investigators have suggested that grain boundary sliding is required for the growth of cavities (Marion et al 1983, Tsai and Raj 1982, Evans 1984). Evidently, higher refractoriness of the intergranular glass phase, caused by oxidation, will make grain boundary sliding harder, and then result in the decrease of strain rate. On the other hand, the creep is restricted by grain contact as grain boundary sliding occurs. As discussed above, contact can be made either at curved surfaces or at

asperities on the grain boundaries. As grain boundary sliding proceeds, the area of contact between grains increases with strain, then more resistance is produced and strain rate decreases continuously with time.

5.3 Influence of Ba Addition on the Grain-Boundary Phase

Both experimental materials are almost identical in terms of microstructure, grain size and porosity, differing only in the composition of the intergranular glass phase. However, they exhibited different creep behaviour under compression. It is suggested that the thickness of the grain-boundary glass film and its viscosity play a very important role in determining the creep mechanisms. In this section, the influence of Ba addition on the thickness and viscosity of the grain-boundary phase will be briefly discussed.

It is not difficult to deduce that the viscosity of the grain-boundary glass phase is decreased due to the addition of Ba. In the undoped material we assume that only pure silica exists at grain boundaries. The grain boundary structure of pure silica network is presented schematically in Fig. 5.5(a). Since Ba^{2+} is known to be a potent silica network modifier, it disrupts the continuity of the network, causing a decrease in viscosity. This disruption is shown schematically in Fig. 5.5(b).

The measured film thickness of the Ba doped material is about 1.4 nm, indicating that the addition of 800 ppm Ba increases the film thickness by about 40%. This result is consistent with the previous report by Tanaka et al (1994b), who studied the calcium concentration dependence of the intergranular film thickness in silicon nitride and found that 450 ppm Ca addition increased the grain-boundary film thickness from about 1 nm to about 1.5 nm.

It is pointed out by Clarke (1987) and co-workers (1993) that the thickness of the intergranular film is determined by a competition between the attractive van der Waals force and the repulsive steric and electrical double layer forces. In the undoped material it is assumed (Tanaka 1994b) that the grain-boundary glass phase is pure silica and the electrical double layer force is neglected at grain boundaries (as shown in Fig. 5.5(a)). The addition of Ba^{2+} to the material disrupts not only the network structure of silica but also the degree of ordering adjacent to the silicon nitride grains (Fig. 5.5(b)). Evidently, this disruption will decrease the magnitude of the steric repulsive force. On the other hand, however, the addition of Ba^{2+} also provides an electrical repulsive force when it adsorbs to the grain surfaces, as shown schematically in Fig. 5.5(c). More additions of Ba^{2+} can be expected to increase the repulsive electrical force. The competition between the effects of a decrease in the steric repulsive force and the development of a

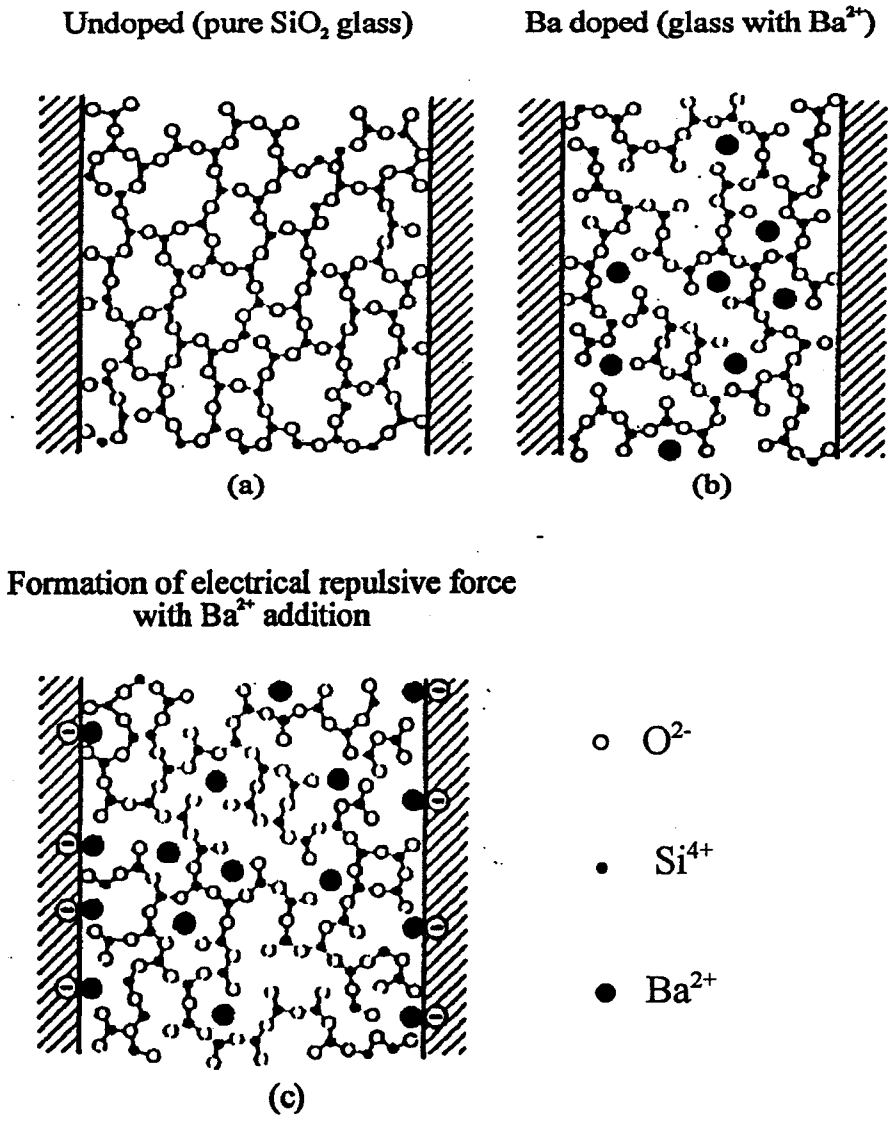

Fig. 5.5 Schematic illustration of changes in the glass structure of the intergranular film with the addition of Ba^{2+} and its influence on the viscosity and the equilibrium film thickness. This was originally used by Tanaka et al (1994b) in analysing the SiO_2+CaO glass system.

repulsive electrical force will determine how the film thickness changes. In the present investigation, it is suggested that the addition of 800 ppm Ba increases the total repulsive force and hence results in the observed increase of the film thickness.

Due to the addition of Ba, the creep mechanisms shift from dissolution-reprecipitation to grain boundary sliding accommodated by cavitation. This perhaps can be attributed to the increase in thickness and decrease in viscosity of the grain-boundary phase, which make the grain boundary sliding and cavitation easier.

CHAPTER 6

CONCLUSIONS AND SUGGESTIONS

6.1 Conclusions

In the present study, the compressive creep behaviour of undoped and 800 ppm Ba doped silicon nitride was investigated at 1400°C under different stresses. Both materials exhibited two creep stages. The difference in strain rate between the two stages is about one order of magnitude, suggesting more than one creep mechanism operates during the creep process.

The first stage of creep is attributed to viscous flow of the grain-boundary glass phase. By statistical analysis of TEM images, it is found that the grain boundary glass phase is redistributed after creep. This provides, for the first time, direct evidence for the viscous flow controlled creep mechanism. Moreover, good agreement is found between the observed creep response and that expected from the viscous flow model.

The mechanisms for the second stage of creep depend on the composition of the materials. The stress exponent of 2.6, large number of strain whorls and obvious cavitation at grain boundaries suggest that the Ba doped material creeps through grain boundary sliding accommodated by cavitation. For the undoped material, the stress exponent of unity and lack of strain whorls and cavitation ascribe creep of this material to dissolution-reprecipitation mechanism.

The addition of 800 ppm Ba to the material increases the thickness and decreases the viscosity of the intergranular phase. It is suggested that this causes the creep mechanism to shift from one to another during the second stage of creep.

6.2 Suggestions for Future Work

The preliminary results of the current work are very encouraging. They not only provide, for the first time, direct evidence for the viscous flow mechanism but also substantiate the previous report on compositional dependence of creep mechanism by using different systems. However, within the limitation of time and resolution of the current TEM studies, much work has to be done in order to have a more comprehensive and clearer understanding of the creep process.

As repeatedly mentioned above, the composition of the intergranular phase is very important in determining the creep behaviour of silicon nitride. Future work should concentrate on this aspect. For instance, we have found a strong compositional dependence of the creep behaviour; the presence of 800 ppm Ba enhanced the intergranular cavitation and shifted the creep mechanism from diffusional to cavitational. It is believed that different levels of Ba addition will help us to have a clearer understanding of the effect of grain bounadry composition on the creep process of silicon nitride materials.

The state of stress (i.e. compression or tension) is one of the important parameters used in evaluating the creep behaviour of glass-containing ceramics such as silicon nitride. The creep behaviour in tension and compression can be totally different (Luecke et al 1994). The current work has only investigated the compressive creep at 1400°C. In future work, the creep behaviour should be evaluated using different states of stress (for example, compression and bending). As we know, one key indicator of the dominant creep mechanism is the creep stress exponent. The activation energy for creep reflects the processes occurring during the creep deformation. Inspection of this data should be helpful in understanding the fundamental mechanisms of high temperature creep. In the future work, therefore, the creep behaviour should be evaluated at different temperatures as well as under

different loads. The stress exponent and the activation energy for creep can be determined using the empirical Norton power law relation (Equ. 4.1).

In the current studies, it is found that grain boundary phase is redistributed after creep. This has been considered as a direct evidence for the viscous flow process during the first stage of creep. However, when this viscous flow process stops is still a question. In the future work, interrupted creep tests should be conducted, and the distribution of grain boundary glass phase should be evaluated as a function of strain under the same testing conditions. Undoubtedly, this will be very helpful in understanding what is really going on during the creep process.

Microstructural analysis is an integral part in order to understand the creep mechanisms. As mentioned above, liquid-phase sintered silicon nitride materials contain an intergranular glass phase, whose composition determines the overall creep behavior of the material. It is now known that the intergranular phase is silicate based and has a thickness of the order of 1 nm. Because the thickness of the intergranular film is so small, direct information from the film is not easy to obtain using a conventional electron microscope (CTEM). This difficulty has hindered a clear understanding of the relationship between the macroscopic phenomenology and the intergranular films. For example, in the current studies,

strain whorls were observed at two-grain boundaries and they were used as evidence of grain boundary sliding and to explain the work hardening phenomenon as due to grain-to-grain contact. Although a strain whorl was observed to occur at two grain contact site (Fig.4.9), whether or not it was representative remains a question for future studies. Clearly, more direct evidence is needed in order to understand how a strain whorl is formed and its relationship with the creep process.

It is suggested that in the future work high resolution and analytical electron microscopy be used to examine the microstructural evolution and to analyze the chemical composition of the grain boundary phase. With these techniques, more direct information can be obtained from the intergranular film and the film thickness can be measured more accurately.

APPENDIX

A WATER-DISPLACEMENT METHOD FOR DETERMINATION OF THE DENSITY OF POROUS CERAMICS

In the present work, a fast, accurate and non-destructive water-displacement method (Pennings et al 1989) has been used to determine the density of the porous Si_3N_4 ceramics. This method is based on three weighings. First the weight W_1 of the dry sample is measured to find the true mass m of the sample (Fig.1 (A)). The sample is then submerged into distilled water and the weight W_2 of the sample in water is obtained (Fig.1 (B)). Finally, the third weight W_3 of the wet sample in air is used to correct for the amount of water which has impregnated into the pores of the sample (Fig.1(C)). If we assume that certain amount of water, V_{water}, has impregnated the pores with total volume of V_p, and the true volume of the sample is V, then the results of the three weighings including the correction for the density of air ρ_{air} can be written as

$$W_1=m-\rho_{air}(V-V_p) \quad (1)$$

$$W_2=m-\rho_{water}(V-V_{water})+\rho_{air}(V_p-V_{water}) \quad (2)$$

$$W_3=m+\rho_{water}V_{water}-\rho_{air}(V-V_p+V_{water}) \quad (3)$$

Equations (1) to (3) lead to the density of the sample

$$\rho=\frac{m}{v}=\rho_{air}+\frac{(\rho_{water}-\rho_{air})(W_1-\rho_{air})}{W_3-W_2} \qquad (4)$$

Since the density of air is small (about 1.00×10^{-3} g/cm^3) compared with the other densities, Equ. (4) can be simplified to

$$\rho=\rho_{water}\frac{W_1}{W_3-W_2} \qquad (5)$$

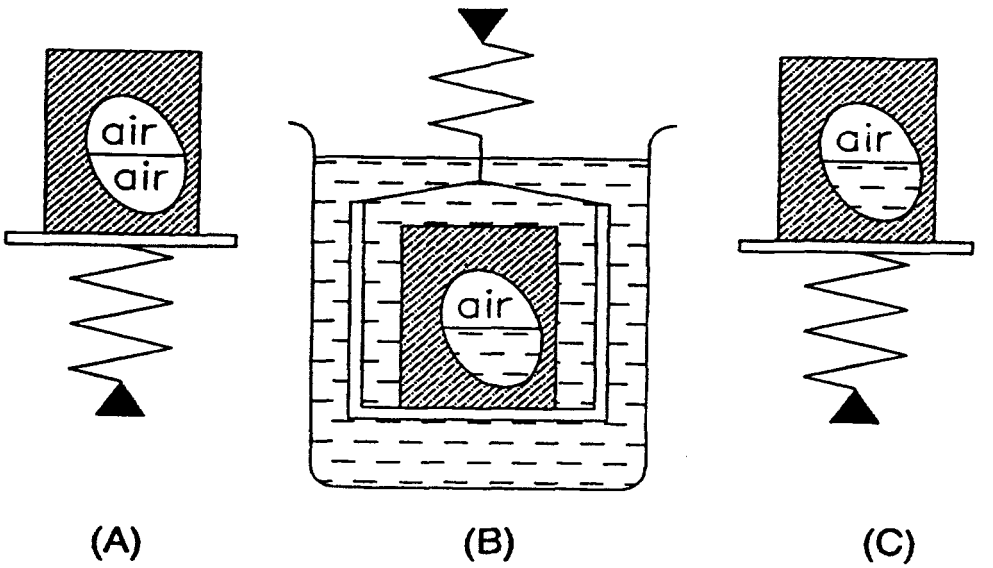

Fig.1 A water displacement method. (A) The weight of the dry sample in air, (B) Submerged in water, the weight W_2 is determined, (C) A third weighing of the "wet" sample.

REFERENCES

Arons R.M.and.Tien J.K., "Creep and Strain Recovery in Hot-Pressed Silicon Nitride" J. Mater. Sci., **15**, 2046-2058 (1980)

Bonnell D.A., Tien T.Y. and Ruhle M., "Controlled Crystallization of the Amorphous Phase in Silicon Nitride Ceramics", J. Am. Ceram. Soc., **70**, 460-465 (1987)

Becher P.F., Hwang H.T., Lin H.T., and Tiegs T.N., "Microstructural Contribution to the Fracture Resistance of Silicon Nitride Ceramics", pp. 87-100 in Proceedings of Workshop: Tailoring of Mechanical Properties of Si_3N_4 Ceramics. Edited by M.J. Hoffmann and G. Petzow, Kluwer Academic Publishers, Dordrecht (1994)

Cahn J.W. and Hilliard J.E., " Free Energy of a Nonuniform System I: Interface Free Energy", J. Chem. Phys., **28**, 258-67 (1958)

Chadwick M.M., "Analytical Electron Microscopy and Creep of Sintered Silicon Nitride", Ph.D.Dissertation, McMaster University, Hamilton, Ontario, Canada (1990)

Chadwick M.M., Jupp R.S. and Wilkinson D.S., "Creep Behaviour of a Sintered Silicon Nitride", J. Am. Ceram .Soc., **76**, 385-396 (1993)

Chadwick M.M., Wilkinson D.S. and Dryden J.R., "Creep Due to a Non-Newtonian Grain Boundary Phase," J. Am. Ceram. Soc., **75**, 2327-2334 (1992)

Cinibulk M.K., Kleebe H.-J., "Effect of Oxidation on Intergranular Phases in Silicon Nitride Ceramics", J. Mater. Sci., **28**, 5775-5782 (1993)

Cinibulk M.K.,Thomas G. and Johnson S.M., "Oxidation Behaviour of Rare-Earth Disilicate-Silicon Nitride Ceramics," J. Am. Ceram. Soc., **75**, 2050-55 (1992)

Clarke D.R., " On the Detection of Thin Intergranular Films By Electron Microscopy", Ultramicroscopy, **4**, 33-44 (1979)

Clarke D.R., " High-Temperature Deformation of a Polycrystalline Alumina Containing an Intergranular Glass Phase", J. Mater. Sci.,**20**, 1321-1332 (1985)

Clarke D.R., " On the Equilibrium Thickness of Intergranular Glass Phases in Ceramic Materials", J. Am. Ceram. Soc.,**70**,15-22 (1987)

Clarke D.R., "High-Temperature Microstructure of a Hot-Pressed Silicon Nitride", J. Am. Ceram. Soc., **72**, 1604-1609 (1989)

Clarke D.R., "The Intergranular Film in Silicon Nitride Ceramics: A Diffuse Interface Approach", pp. 291-301 in Proceedings of Workshop: Tailoring of Mechanical Properties of Si_3N_4 Ceramics. Edited by M.J. Hoffmann and G. Petzow, Kluwer Academic Publishers, Dordrecht (1994)

Clarke D.R., Shaw T.M., Philipse A.P., and Horn R.G., "Possible Electrical Double-Layer Contribution to the Equilibrium Thickness of Intergranular Glass Films in Polycrystalline Ceramics", J. Am. Ceram. Soc., **76**, 1201-204 (1993)

Coble R.L., "A Model for Boundary Diffusion Controlled Creep in Polycrystalline Materials", J. Appl. Phys., **43**, 1679-1682 (1963)

Din S.U., Nicholson P.S., "Creep of Hot-Pressed Silicon Nitride ", J. Mater. Sci., **10**, 1375-80 (1975)

Drucker D.C., "Engineering and Continuum Aspects of High-Strength Materials", pp.795-833 in High Strength Materials. Edited by V.F.Zackay,Wiley Press, New York (1965)

Dryden J.R., Kucerovshy D., Wilkinson D.S. and Watt D.F., "Creep Deformation Due to a Viscous Grain Boundary Phase", Acta Metall, **37**,2007-2015 (1989)

Dryden J.R. and Wilkinson D.S., "Effect of Grain Aspect Ratio on Creep Due to a Viscous Grain Boundary Phase", to be published (1995)

Durney D.W., "Solution-Transfer, an Important Geological Deformation Mechanism", Nature, **235**, 315-317 (1972)

Evans A.G.and Sharp J.V., "Microstructural Studies on Silicon Nitride", J.Mater.Sci., 6,1292-1302 (1971)

Evans H.E., "Mechnisms of Creep Fracture", Elsevier Applied Science, London (1984)

Gurther M. and Grathwohl G., in Proceedings of the Fourth International Conference on Creep and Fracture of Engineering Materials and Structures, Institute of Metals, London (1990)

Haig S., Cannon W.R., Whalen P.J., "Anelastic Recovery in Crept Silicon Nitride", pp. 1008-1023 in Ceramic Engineering & Science Proceedings. Edited by J.B. Wachtman, The American Ceramic Society, Westerville, OH (1992)

Herrring C., "Diffusional Viscosity of a Polycrystalline Solid", J. Appl. Phys., 21,437-445 (1950)

Hockey B.J., Wiederhorn S.M., Liu W., Baldoni J.G. and Buljan S.-T., "Tensile Creep of Whisker-Reinforced Silicon Nitride", J.Mater. Sci. 26, 3931-3939 (1991)

Hohnke H. and Tien T.Y., " Solid-Liquid Reactions in Part of the System Si, Al, Y/N,O", pp.101-110 in Progress in Nitrogen Ceramics. Edited by F.L.Riley, Martinus Nijhoff, The Hague (1983)

Hull D., and Rimmer D.E., "The Growth of Grain-Boundary Voids Under Stress", Phil. Mag. 4, 673-687 (1959)

Jakus K.,Wiederhorn S.M. and Hockey B.J., " Nucleation and Growth of Cracks in Vitreous-Bounded Aluminum Oxide at Elevated Temperatures", J. Am. Ceram.Soc., 69,725-731(1986)

Kessler H., Kleebe H.-J., Cannon R.W. and Pompe W., " Effect of Internal Stress on Crystallization of Intergranular Phases in Ceramics," Acta Matell. Mater., 40, 2233-2245 (1992)

Kleebe H.-J., unpublished work (1994a)

Kleebe H.-J., Bruley J. and Ruhle M., "HREM and AEM Studies of Yb_2O_3-Fluxed Silicon Nitride Ceramics with and without CaO Addition", J. Euro. Ceram. Soc.,**14**,1-11(1994b)

Kleebe H.-J., Cinibulk M.K.,Cannon R.M. and Ruhle M., "Statistical Analysis of the Intergranular Film Thickness in Silicon Nitride", J.Am.Ceram.Soc.,**76**,1969-1977 (1993a)

Kleebe H.-J.,Cinibulk M.K.,Tanaka I., Bruley J., Cannon R.M., Clarke D.R., Hoffmann M.J. and Ruhle M.,"High-Resolution Electron Microscopy Observations of Grain-Boundary Films in Silicon Nitride Ceramics", pp.65-78 in Silicon Nitride Ceramics: Scientific and Technological Advances, Materials Research Society Symposium Proceedings, 287. edited by I.-W. Chen, P.F.Becher, M.Mitomo, G.Petzow and T.-S. Yen. Materials Research Society, Pittsburgh, PA (1993b)

Kleebe H.-J., Cinibulk M.K. , Tanaka I., Bruley J. , Vetrano J.S., and Ruhle M., "High Resolution Electron Microscopy Studies on Silicon Nitride Ceramics", pp. 259-274 in Proceedings of Workshop: Tailoring of Mechanical Properties of Si_3N_4 Ceramics. Edited by M.J. Hoffmann and G. Petzow, Kluwer Academic Publishers, Dordrecht (1994c)

Kosowsky R., "Cyclic Fatigue of Hot-Pressed Si_3N_4", J.Am.Ceram.Soc., **56**, 531-535 (1973)

Kossowsky R., Miller D.G. and Diaz E.S., "Tensile and Creep Strengths of Hot-Pressed Si_3N_4", J. Am. Ceram.Soc.,**74**, 915-921 (1991)

Lange F.F., "Relation Between Strength, Fracture Energy, and Microstructure of Hot-Pressed Si_3N_4," J. Am. Ceram. Soc., **56**, 518-522 (1973)

Lange F.F., Clarke D.R. and Davis B.I., "Compressive Creep of Si_3N_4/MgO Alloys", Part 2 Source of Viscoelastic Effect, J. Mater. Sci., **15**, 611-615 (1980a)

Lange F.F., Davis B.I. and Clarke D.R., "Compressive Creep of Si_3N_4/MgO Alloys", Part 1, Effect of Composition, J. Am. Ceram. Soc.,**15**, 601-610 (1980b)

Lange F.F., Davis B.I. and Clarke D.R., "Compressive Creep of Si_3N_4/MgO Alloys", Part 3, Effects of Oxidation Induced Compositional Change, J. Am. Ceram. Soc.,**15**, 616-618 (1980c)

Lee W.E., Drummond C.H., Hilmas G.E., Kiser J.D., Sanders W.A., "Microstructural Evolution on Crystallizing the Glass Phase in a 6 weight % Y_2O_3-Si_3N_4 Ceramic", Ceram. Eng. Sci. Proc., **19**, 1355-65 (1988)

Lewis M.H., Bhatti A.R., Lumby R.J. and North B., " Microstructure of Sintered Si-Al-O-N Ceramics", J. Mater. Sci., **15**, 103-113 (1980)

Lewis M.H., Leng-Ward G. and Jasper C., "Sintering additive Chemistry in Controlling Microstructure and Properties of Nitride Ceramics" pp. 1019-1033 in Ceramic Transactions, Vol. 1. Edited by G.L. Messsing, E.R. Fuller and Jr. H. Hausner. The American Ceramic Society, Westerville, OH (1988)

Loehman R.E., " Structure, Formation , and Stability of Oxynitride Glasses," pp. 167-173 in Proceedings of Workshop: Tailoring of Mechanical Properties of Si_3N_4 Ceramics. Edited by M.J. Hoffmann and G. Petzow, Kluwer Academic Publishers, Dordrecht (1994)

Luecke W.E. and Wiederhorn S.M., "Tensile and Compressive Asymmtry in Silicon Nitride", pp.587-91 in Silicon nitride'93. Edited by M.Hoffmann, G. Petzow and P. F. Becker, Trans Tech., Aedermannsdorf, Switzerland (1994)

Luecke W.E., Wiederhorn S.M., Hockey B.J., Kranse R., Jr. and Long G.G., "Cavitation Contributes Substantially to Tensile Creep in Silicon Nitride", submitted to J.Am. Ceram.Soc.(1994)

Marion J.E., Evans A.G. and Drory M.D., "High Temperature Failure Initiation in liquid Phase Sintered Materials", Acta metall, **31**,1445-1457 (1983)

Marion J.E., Hsueh C.H. and Evans A.G., "Liquid Phase Sintering of Ceramics", J. Am. Ceram. Soc., **70**, 708-713 (1987)

Nabarro F.R.N., Report on a conference on the Strength of Metals, Phys. Soc. London (1948)

Ness J.N., Stobbs W.M. and Page T.F., " A TEM Fresnel Diffraction-Based Method for Characterizing Thin Grain-Boundary and Interfacial Films, Phil. Mag. A, **54**, 679-702 (1986)

Page R.A., Lankford J., Chan K.S.,Handman-Rhyne K. and Spooner S., "Creep Cavitation in Liquid-Phase-Sintered Alumina", J. Am.Ceram. Soc.,**70**, 137-145 (1987)

Pennings E.C.M., and Grellner W. , "Precise Non-destructive Determination of the Density of Porous Ceramics", J. Am. Ceram. Soc. **72**, 1268-70 (1989)

Pharr G.M and Ashby M.F., "On Creep Enhanced by a Liquid Phase", Acta Metall, **31**, 129-138 (1983)

Pierce L.A., Mieskowski D.M. and Sanders W.A., "Effect of Grain-Boundary Crystallization on the High-Temperature Strength of Silicon Nitride," J. Mater. Sci., **21**, 1345-48 (1986)

Raj R., " Creep in Polycrystalline Aggregates by Matter Transport Through a Liquid Phase", J. Geophys. Res. **87B**, 4731-4739 (1982)

Raj R.and Chyung C.K., "Solution-Precipitation Creep in Glass Ceramics", Acta Metall, **129**, 159-166 (1981)

Tanaka I., Bruley J., Gu H., Hoffmann M. J., Kleebe H.-J. Cannon R.M., Clarke D.R., and Ruhle M., " Composition and Thicknesses of Grain Boundary Films in Ca-Doped Silicon Nitride Ceramics", pp. 257-289 in Proceedings of Workshop: Tailoring of Mechanical Properties of Si_3N_4 Ceramics. Edited by M.J. Hoffmann and G. Petzow, Kluwer Academic Publishers, Dordrecht (1994a)

Tanaka I. , Igashira K.-I., Okamoto T., Niihara K. and Cannon R. M., "High-Temperature Fracture Mechanism of Low-Ca-Doped Silicon Nitride", J. Am.Ceram. Soc., **78**, 673-679 (1995)

Tanaka I., Kleebe H.-J., Cinibulk M.K., Bruley J.,Clarke D.R., and Ruhle M., "Calcium Concentration Dependence of the Intergranular Film Thickness in Silicon Nitride", J. Am. Ceram.Soc. **77**, 911-914 (1994b)

Thorel A., Laval J.Y., Broussaud, Sagey G. De., Schiffmacher G., "Grain Boundary Structure of SiAlON'S for Thermomechanical Applications," pp. 819-826 in Proceedings of JIMIS-4 (1986)

Tighe N. J., "The Structure of Slow Crack Interfaces in Silicon Nitride", J. Mater. Sci., **13**, 1455-63 (1978)

Tsai R. L. and Raj R., "Creep Fracture in Ceramics Containing Small Amounts of a Liquid Phase", Acta metall. **30**, 1043-1058 (1982)

Wiederhorn S.M., Hockey B.J., Cranmer D.C.and Yeckley R., "Transient Creep Behaviour of Hot Isostatically Pressed Silicon Nitride", J. Mater. Sci., **28**, 445-53 (1993)

Wiederhorn S.M., Hockey B.J., Krause R.F., Jakus K., " Creep and Fracture of a Vitreous -Bonded Aluminum Oxide", J. Mater. Sci., **21**, 810-824 (1986)

Wiederhorn S.M., Luecke W.E., Hockey B.J. and Long G.G., " Creep Damage Mechanisms in Si_3N_4", pp. 305-326 in Proceedings of Workshop:Tailoring of Mechanical Properties of Si_3N_4 Ceramics. Edited by M.J.Hoffmann and G.Petzow, Kluwer Academic Publishers, Dordrecht (1994)

Wild S., Grieveson P., Jack H. and Latimer M., p.377 in Special Ceramics 5. Edited by P. Popper, British Ceramic Research Association, Stoke-On-Trent, England (1972)

Wilkinson D.S.,"Creep Mechanism in Silicon Nitride Ceramics", pp. 327-338 in Proceedings of Workshop: Tailoring of Mechanical Properties of Si_3N_4 Ceramics. Edited by M.J.Hoffmann and G.Petzow, Kluwer Academic Publishers, Dordrecht (1994)

Ziegler G., Heinrich J. and Wotting G., "Review: Relationship Between Processing, Microstructure and Properties of Dense and Reaction Bonded Silicon Nitride," J. Mater. Sci., **22**, 3014-86 (1987)